Cell Chemical Biology

Glucose metabolism and oxygen availability govern reactivation from latency of the human retrovirus HTLV-1

--Manuscript Draft--

Manuscript Number:	CELL-CHEMICAL-BIOLOGY-D-17-00210R2
Full Title:	Glucose metabolism and oxygen availability govern reactivation from latency of the human retrovirus HTLV-1
Article Type:	Research Article
Keywords:	HTLV-1; latency; virus; metabolism; hypoxia; glucose; 2-oxoglutarate; HIF hydroxylase; epigenetic regulation
Corresponding Author:	Charles R M Bangham, ScD Imperial College London London, UNITED KINGDOM
First Author:	Anurag Kulkarni, MBBS, PHD
Order of Authors:	Anurag Kulkarni, MBBS, PHD
	Manuel Mateus, MSc
	Cyrille C. Thinnes, PhD
	James S. McCullagh, PhD
	Christopher J. Schofield, PhD
	Graham P. Taylor, MBBS, PhD
	Charles R M Bangham, ScD
Abstract:	The human retrovirus HTLV-1 causes a haematological malignancy or neuroinflammatory disease in ~10% of infected individuals. HTLV-1 primarily infects CD4+ T-lymphocytes and persists as a provirus integrated in their genome. HTLV-1 appears transcriptionally latent in freshly-isolated cells; however, the chronically active anti-HTLV-1 cytotoxic T-cell response observed in infected individuals indicates frequent proviral expression in vivo. The kinetics and regulation of HTLV-1 proviral expression in vivo are poorly understood. By using hypoxia, small molecule hypoxia mimics and inhibitors of specific metabolic pathways, we show that physiologically relevant levels of hypoxia, as routinely encountered by circulating T-cells in the lymphoid organs and bone marrow, significantly enhances HTLV-1 reactivation from latency. Furthermore, culturing naturally infected CD4+ T-cells in glucose-free medium or chemical inhibition of glycolysis or the mitochondrial electron transport chain strongly suppresses HTLV-1 plus-strand transcription. We conclude that glucose metabolism and oxygen tension regulate HTLV-1 proviral latency and reactivation in vivo.
Suggested Reviewers:	Patrick Maxwell phm29@medschl.cam.ac.uk Expert on hypoxia biology
	Mridul Mukherji mukherjim@umkc.edu Expert on 2-OG oxygenase enzymes
	Marc Sitbon marc.sitbon@igmm.cnrs.fr Authority on metabolism and human retroviruses
	Naomi Taylor naomi.taylor@igmm.cnrs.fr Expert on glucose metabolism and human retroviruses
Opposed Reviewers:	

Powered by Editorial Manager® and ProduXion Manager® from Aries Systems Corporation

Faculty of Medicine
Imperial College London

Wright-Fleming Institute,
St Mary's campus,
Norfolk Place,
London W2 1PG,
Tel: +44 (0)20 7594 3730
Fax: +44 (0)20 7402 0653

c.bangham@imperial.ac.uk
www.imperial.ac.uk

Charles R. M. Bangham
PhD ScD MRCP FRCPath FMedSci
Professor of Immunology
Head, Division of Infectious Diseases

1 August 2017

Dear Dr. Suga,

We write to submit the final revised version of our paper on the metabolic factors that regulate latency of the human retrovirus, HTLV-1, also known as the human leukaemia virus.

We have updated the manuscript to attend to the remaining points; we have also included the conflict of interest form and a graphical abstract.

I believe it is now complete; please let me know if any further details are needed.

Yours sincerely,

Charles R M Bangham

REVIEWERS' COMMENTS

Reviewer #1: The study by Kulkarni et al. presents important and novel information on the role of oxygen concentrations and glucose metabolism in the reactivation of HTLV-1. The group of Charles Bangham extend critical studies from their lab, convincingly showing that physiological hypoxia enhances human retrovirus HTLV-1 plus-strand transcription without changing minus-strand transcription (sHBZ). Notably though, the authors find that stabilization of HIF1a in the context of an inhibition of 2-OG-dependent enzymatic processes (by DMOG) has opposing effects, decreasing plus-strand transcripts while sHBZ transcripts are increased. They go on to perform an extensive number of analyses on the methylation and metabolic status of these HTLV-1-infected PBMCs in the different conditions. These experiments reveal the importance of aerobic glycolysis, but not oxidative phosphorylation, in the efficient transcription of TAX. The authors present a huge amount of complex data and should be commended for their study.

While potentially outside the scope of the study, the authors may want to comment on the following points in a final version of the manuscript:

-The authors convincingly show that at early time points, DMOG inhibits Tax transcription but there is no upregulation of sHBZ. Furthermore, they find that at that time point, VEGF levels are not yet increased, strongly suggesting that HIF1a is probably not yet stabilized. Thus, do the authors propose that sHBZ transcription is dependent on HIF1a stabilization together with an inhibition of aKG-dependent enzymatic activities?
Treatment with the specific HIF stabiliser IOX2 did not result in an increase in *sHBZ* transcription levels, which rules out the involvement of HIF in inducing minus-strand HTLV-1 transcription (Figure 2B). On the contrary, a small but significant inhibition of sHBZ transcription was observed in response to IOX2 treatment. The reason for this effect is unknown but could be a 'secondary' resulting from the known upregulation of multiple HIF-target genes in response to IOX2 treatment.

Is sHBZ increased under conditions where glycolysis is inhibited?
There was no significant difference in *sHBZ* transcription levels when compared to corresponding controls upon treatment with inhibitors of glycolysis (iodoacetate, 0 mM glucose, 2-deoxyglucose), TCA cycle inhibitor (arsenite) or TCA cycle inducers (pyruvate, galactose). These data are shown in the newly added Supplementary Figure S4.

-All mRNA quantifications are performed relative to 18S transcripts. Under conditions where glycolysis is inhibited, is there a change in "housekeeping" genes such as actin?
18S rRNA has been found to be one of the most stable housekeeping genes in T-lymphocytes and its levels remained constant even after lymphocyte activation (Bas et al., 2004). On the contrary, beta-actin and GAPDH levels fluctuated markedly in response to activation in T-lymphocytes (Bas et al., 2004). In the studies carried out in this manuscript, 18S rRNA levels remained constant in response to varied conditions (hypoxia, glycolysis and TCA cycle modulations).

Minor:
-The authors may want to consider incorporating information in the first paragraph of the intro into the last paragraph of the intro.

Thank you for this suggestion. We have now incorporated the information in the first paragraph of the introduction into the last paragraph, and the result is more succinct.

-It might be helpful to separate Figs 3A and 3B as the former is at 2h and the latter is assessed after an overnight culture. Moreover, the increase in 3HBZ is related to the data presented in figure 2C.
Figure 3B and C have been moved to supplementary data. They are now supplementary figures S3B and C.

-Figure 4 was difficult to read in the downloaded version (fuzzy) and this reviewer wonders whether depletion should be on the left and induction on the right. Furthermore, increases in glyceraldehyde-3-phosphate and alpha-D-glucose 6-phosphate may be related to the increased early steps in the pentose phosphate pathway. As such, grouping them together with the PPP, rather than glycolysis, might provide a more homogeneous explanation of decreased glycolysis and increased early PPP intermediates.
The resolution of Figure 4 has been increased. As recommended, depletion is now shown on the left and induction on the right. Glyceraldehyde-3-phosphate and alpha-D-glucose 6-phosphate have been grouped with the pentose phosphate pathway, rather than glycolysis.

Reviewer #2: This report by Kulkarny et al. comprises two parts of very different importance. In the first part, the authors go into great length to evaluate the potential role of epigenetic modifications in the activation of HTLV-1 tax transcripts that they observed in patient PBMC placed in low oxygen tension (1-2%). Although the authors could show some significant histone modification associated with promoter function (H3K4Me3) on the proviral 5'LTR (viral promoter) and tax (located approximately 2/3rd into the provirus) regions, no convincing change, marking active transcription (H3K36me3), could be demonstrated in gag (located in the 5' first third of the virus, between the 5'LTR and tax).
ChIP assays for only the 5'-LTR junction, Gag and 3'-LTR Jn were provided in the version before. In the revised manuscript, ChIP enrichment in all the regions of the HTLV-1 provirus including *pol*, *env*, *vCTCF* and *tax* are shown for H3K4me3, H3K36me3 (Figure 1B, C) and H3K27me3 (Figure S1).

There was a significant increase in the H3K4me3 mark upon activation under both 1% and 20% oxygen conditions, in all the regions of the HTLV-1 provirus from the 5'-LTR junction up to the *vCTCF* region This observation is in agreement with a recent report (Satou et al., 2016) which identifies the *vCTCF* region as an epigenetic border, putatively established by the binding of CTCF to the HTLV-1 provirus.

There was also an increase in the H3K36me3 mark upon viral reactivation under both 1% and 20% oxygen, in the 5'-LTR junction, *gag*, *pol*, *env*, *vCTCF*, *tax* and 3'-LTR junction regions However, the increase observed in the *gag* and *pol* regions was not statistically significant, perhaps because these regions were highly enriched in the H3K36me3 mark even at time 0 in immediately fixed PBMCs.

Since low oxygen tension evoked a role for HIF complexes, the authors tested the dimethyloxalylglycine (DMOG), a stabilizing agent of HIF-1 alpha, as a modulator of HTLV transcription. They go into a thorough and convincing demonstration that DMOG action on

HTLV transcription was not dependent on HIF or epigenetic modifications.
In the second part of their report, the authors went on to tackle the metabolic impact of DMOG in patient PBMC by mass spec analyses to unveil major modifications within what they could group into 6 main metabolic pathways. They experimentally relate these effects to describe a new property of DMOG as a glycolytic inhibitor.
They further tested this observation by assessing glucose deprivation, 2-DG (a glucose analogue) and pyruvate complementation to most convincingly make this point. Importantly, they did not see a major role of the TCA cycle in the HTLV tax activation in PBMC placed under hypoxia. Nevertheless, they went on to examine the effect of mitochondrial electron transport chain inhibitors to unveil an additional role of ETC on HTLV tax "hypoxic transcription".
This study has the considerable merit of using solely patient PBMC, in conditions that are likely to mirror some aspects of the lymphatic system, with low oxygen pressure. Although physiological hypoxia has been used in numerous studies on cell metabolism, to my knowledge, this is the first report to assess its its impact on HTLV patient PBMC. The demonstration of a key role for glycolysis in HTLV tax transcription is of paramount interest with regards to our understanding of HTLV activation from latency. The findings reported in the second part of the manuscript also bear importance with regards to HIV cell reservoir activation.
In conclusion, for a more impactful and clearer message, I strongly recommend to eliminate most, if not all of the negative results in the first part of the manuscript, for which I have other reticence (see below).
Figure 2B and C have been moved to supplementary data section and are now figures S3B and C

Other comments

1- Although the authors convincingly show that hypoxia increases tax RNA production, this does not necessarily correspond to an active viral production. Have the authors tested the activation of unspliced full-length RNA, or viral protein products, if not virions? Similarly, have they followed GLUT1 or expression of other GLUTs in patient PBMC?
The aim of this study was to analyse the initial effects on spontaneous HTLV-1 transcription of modulations in the host microenvironment. In follow-up studies it will indeed be of interest to quantify unspliced full-length RNA and protein products. Similarly, changes in GLUT1 expression in PBMCs would be very insightful but were also beyond the scope of the current study.

2- The scenario offered by the authors of a viral activation and production under low oxygen pressure remains perplexing, as those conditions are not rarely encountered in lymphatic organs. It therefore remains difficult to understand the long latency (decades) and relatively low prevalence (5%) of high viral loads in HTLV carriers.
A strong, chronically activated cytotoxic T-cell response to HTLV-1 antigens has always been detected in HTLV-1 infected individuals. The rate at which host CTLs kill HTLV-1 infected cells is one of the most decisive determinants of proviral load in infected individuals (see Bangham 2009: Eur. J. Immunol. **39**, 1700-1712 for a review). The CTL response to HTLV-1, in combination with viral factors including the integration site of the provirus and its orientation in relation to nearby host cellular genes, plays a critical role in limiting the proviral load in HTLV-1 carriers.

3- Epigenetic changes that are supposed to accompany viral activation are not clear for the gag region, unless the H3K4me3 modification is sufficient for transcriptional activity. Therefore, it is difficult to envision the pattern of epigenetic modification proposed as compatible with full provirus transcription. The gag region sitting between the 5'LTR and tax does not seem to follow the same scenario. Overall, even in the absence of treatment with inhibitors, the epigenetics data are not overtly convincing. Fig 3B and C show non-significant variations for the histone signatures due to large error bars (compare with tighter error bars of fig 1).

As mentioned above, epigenetic changes in all the regions of the HTLV-1 provirus are now shown in the revised manuscript version. The changes in H3K4me3 and H3K36me3 in all the regions of the provirus are consistent with full provirus activation. Although there was an increase in H3K36me3 in the *gag* and *pol* regions of the provirus upon activation, it was not statistically significant, perhaps because these regions are highly enriched in that activation mark even at time 0 in immediately fixed PBMCs. We have added a sentence to the revised manuscript to clarify this point.

The larger error bars in supplementary figures S3 B, C and D are likely due to 'epigenetic' variations observed between HTLV-1-infected individuals. Although the degree of enrichment varies from case to case, no consistent trend was observed in the changes in response to DMOG. We therefore conclude that DMOG does not play a role in changing the epigenetic signature of the HTLV-1 provirus.

4- It is not clear to me why methylstat and JIB-04 methylase inhibitors would have opposite effects on VEGF transcription?

It is known that Methylstat inhibits angiogenesis and *VEGF* transcription (Cho et al., 2014). However no such study has been carried out in relation to JIB-04. It is interesting that these two compounds have opposing effects on *VEGF* transcription which further highlights the importance of using multiple inhibitors targeting a single pathway to exclude off-target and secondary effects. A comment has been made to that effect in the manuscript.

5- Page 10: The lack of impact on sHBZ transcription does not necessarily mean a lack of a role for sHBZ. DMOG may have also a direct or indirect impact on sHBZ protein pools.

We agree, and a comment to highlight this has been made in the manuscript.

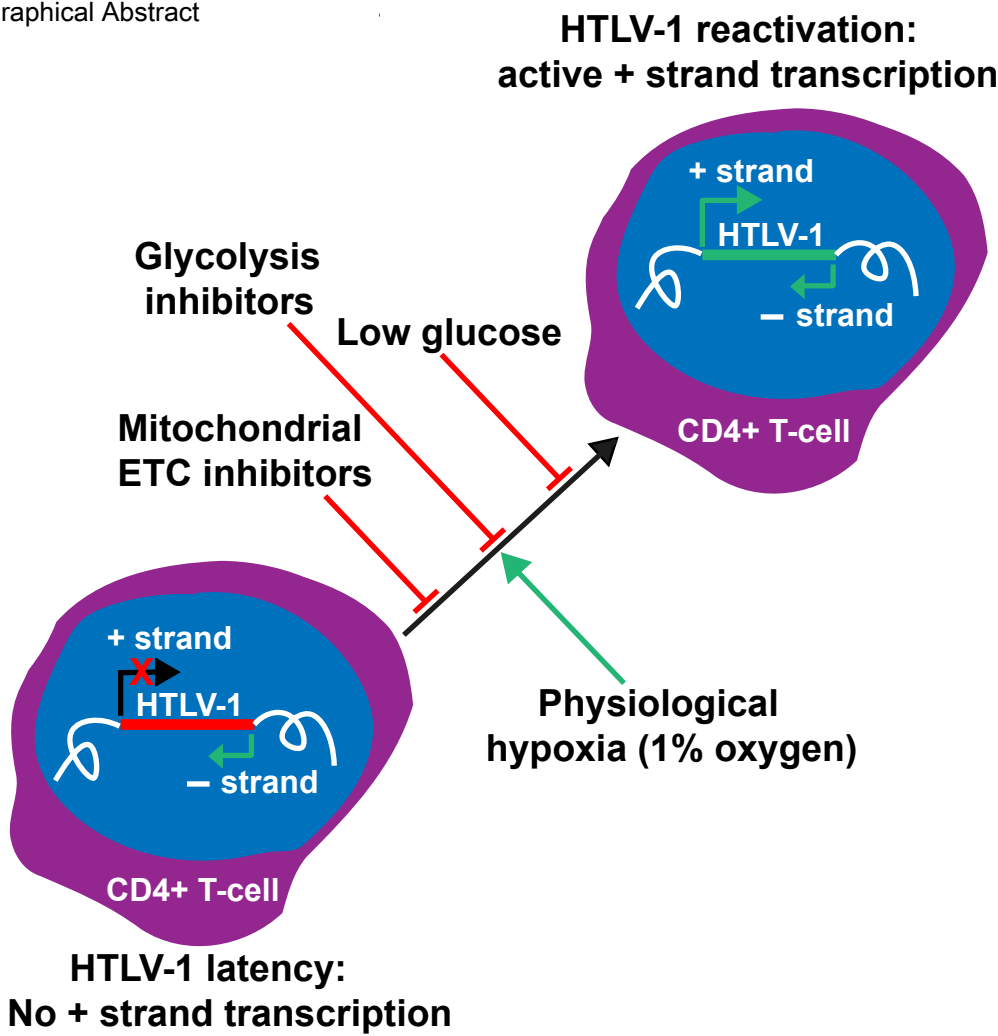
Bibliography

Bas, A., Forsberg, G., Hammarstrom, S., and Hammarstrom, M.L. (2004). Utility of the housekeeping genes 18S rRNA, beta-actin and glyceraldehyde-3-phosphate-dehydrogenase for normalization in real-time quantitative reverse transcriptase-polymerase chain reaction analysis of gene expression in human T lymphocytes. Scand J Immunol *59*, 566-573.

Cho, Y., Kim, K.H., Cho, Y.S., Xu, W.Q., Wang, X., and Kwon, H.J. (2014). A histone demethylase inhibitor, methylstat, inhibits angiogenesis in vitro and in vivo. Rsc Advances *4*, 38230-38233.

Satou, Y., Miyazato, P., Ishihara, K., Yaguchi, H., Melamed, A., Miura, M., Fukuda, A., Nosaka, K., Watanabe, T., Rowan, A.G., et al. (2016). The retrovirus HTLV-1 inserts an ectopic CTCF-binding site into the human genome. Proc Natl Acad Sci U S A *113*, 3054-3059.

Graphical Abstract



Title:

Glucose metabolism and oxygen availability govern reactivation from latency of the human retrovirus HTLV-1

Authors:

Anurag Kulkarni[1], Manuel Mateus[1], Cyrille C. Thinnes[2], James S. McCullagh[2], Christopher J. Schofield[2], Graham P. Taylor[1], and Charles R.M. Bangham[1,3]

[1]Section of Virology, Department of Medicine, Imperial College, London W2 1PG, United Kingdom.

[2]Chemistry Research Laboratory, Department of Chemistry, University of Oxford, Mansfield Road, Oxford, United Kingdom.

[3]Lead contact.

***Correspondence:** c.bangham@imperial.ac.uk

Summary:

The human retrovirus HTLV-1 causes a haematological malignancy or neuroinflammatory disease in ~10% of infected individuals. HTLV-1 primarily infects $CD4^+$ T-lymphocytes and persists as a provirus integrated in their genome. HTLV-1 appears transcriptionally latent in freshly-isolated cells; however, the chronically active anti-HTLV-1 cytotoxic T-cell response observed in infected individuals indicates frequent proviral expression in vivo. The kinetics and regulation of HTLV-1 proviral expression in vivo are poorly understood. By using hypoxia, small molecule hypoxia mimics and inhibitors of specific metabolic pathways, we show that physiologically relevant levels of hypoxia, as routinely encountered by circulating T-cells in the lymphoid organs and bone marrow, significantly enhances HTLV-1

reactivation from latency. Furthermore, culturing naturally infected $CD4^+$ T-cells in glucose-free medium or chemical inhibition of glycolysis or the mitochondrial electron transport chain strongly suppresses HTLV-1 plus-strand transcription. We conclude that glucose metabolism and oxygen tension regulate HTLV-1 proviral latency and reactivation in vivo.

Key words:

HTLV-1, latency, virus, metabolism, hypoxia, glucose, 2-oxoglutarate, HIF hydroxylase, epigenetic regulation.

Highlights:

- Physiological (1%) hypoxia enhances human retrovirus HTLV-1 plus-strand transcription.
- HTLV-1 transcription is hypoxia-regulated but HIF-independent.
- Inhibition of glycolysis or mitochondrial ETC supresses HTLV-1 transcription.
- Extracellular glucose concentration influences HTLV-1 reactivation from latency.

In brief:

Kulkarni et al. show that fluctuations in glucose metabolism and oxygen availability ex vivo, as encountered routinely by circulating CD4+T-cells in vivo, govern spontaneous reactivation of human retrovirus HTLV-1 from latency.

Introduction

HTLV-1 is a human retrovirus that primarily infects $CD4^+$ T-lymphocytes. It is a single-stranded positive-sense RNA virus that reverse transcribes its RNA genome and integrates the resulting dsDNA copy of its genome into the host cellular chromatin (as a provirus), thereby establishing a persistent infection in the cells. It is estimated that 5 to 10 million people worldwide are HTLV-1 carriers. HTLV-1 infection is asymptomatic in most cases. In a subset of infected individuals (~5% to 10%), however, HTLV-1 infection progresses to either a $CD4^+$ T-cell malignancy known as Adult T-cell Leukaemia/Lymphoma (ATL), or to HTLV-1 associated myelopathy (HAM), a progressive inflammatory disease of the spinal cord.

HTLV-1 infection is considered to be largely latent in infected individuals, because the viral structural RNA and protein products are usually undetectable in freshly isolated infected peripheral blood mononuclear cells (PBMCs) (Hanon et al., 2000; Rende et al., 2011). However, the presence of a sustained chronically activated cytotoxic T-cell response against HTLV-1 antigens, in infected individuals, suggests that the immune system frequently encounters newly-synthesized viral antigens within the body (Bangham, 2009; Hanon et al., 2000). Hence it is important to understand the mechanisms that regulate the latency, reactivation and productive infection of HTLV-1 *in vivo*. This understanding might suggest strategies to reactivate the dormant virus and make it accessible to attack by the immune system and antiretroviral drugs.

Previous work on HTLV-1 proviral latency and reactivation has largely focused on identifying the viral factors involved, such as the HTLV-1 integration site (Melamed et al., 2013). Spontaneous reactivation of the provirus is associated with integration in

transcriptionally active euchromatin, in opposite transcriptional orientation of the nearest host gene and within 100 bases of certain transcription factor binding sites (Gillet et al., 2011; Melamed et al., 2013). Recently, it has been shown that the HTLV-1 provirus binds the key host chromatin insulator-binding transcription factor CTCF (CCCTC binding factor) (Satou et al., 2016). The functional consequences of this binding are not yet clear; we hypothesize that CTCF binding regulates proviral transcription, local chromatin structure and alternative splicing of mRNA.

Different cell types are exposed to widely differing oxygen tension in vivo. While pulmonary alveolar cells experience oxygen concentrations of ~15%, embryonic, neural, mesenchymal, and haematopoietic stem cells are exposed to profoundly hypoxic environments (~1% O_2) (Ivanovic, 2009; Mohyeldin et al., 2010). Viruses have evolved different strategies either to counter the detrimental effects of oxygen variations or to exploit hypoxic cellular metabolism to their own advantage, thereby enabling them to infect different cell types and replicate or persist in the host (Ebbesen and Zachar, 1998; Morinet et al., 2013). Circulating $CD4^+$ T-cells are of special interest as they encounter frequent changes in oxygen tension and extracellular fluid, and contact several different cell types. We set out to test the hypothesis that these extracellular stresses and changing microenvironment influence transcription of the HTLV-1 provirus. To this end we took two complementary approaches. First, in a 'top-down' approach we studied the effects on HTLV-1 transcription of cellular stresses routinely encountered within the body such as physiological hypoxia and nutrient limitation. Secondly, in a 'bottom-up' approach we identified specific epigenetic and transcriptional changes in the provirus in response to specific inhibitors of cellular metabolic and stress-response pathways that are known to play an important role in cellular adaptation to the external environment.

To minimize artefacts due to in vitro selection and adaptation, we employed primary PBMCs isolated from HTLV-1-infected individuals to study the effects of various stresses and inhibitors on HTLV-1 reactivation from latency. Plus-strand HTLV-1 gene expression is typically undetectable in fresh PBMCs obtained from HTLV-1-infected individuals, but there is a strong spontaneous increase in the expression of Tax, the viral transactivator of plus-strand gene transcription, within a few hours of isolation (Hanon et al., 2000; Rende et al., 2011). An increase in Tax transcription can also be observed in cultures of whole blood obtained from HTLV-1-infected individuals (Hanon et al., 2000). These observations suggest that changes in the extracellular microenvironment have an important impact on HTLV-1 proviral transcription.

Results

Hypoxia enhances HTLV-1 plus-strand transcription

The concentration of oxygen in venous blood ranges from 5% to 10%, and in air at sea-level is ~20%. Previous studies of gene expression in HTLV-1-infected patients' PBMCs have been carried out under ambient atmospheric conditions (~20% oxygen). However, lymphocytes spend most of their time in the highly hypoxic environment of the lymph circulation or solid lymphoid organs (1% to 2% oxygen) (Hangai-Hoger et al., 2007; Tsai et al., 2004). To study the impact of physiological hypoxia on the integrated HTLV-1 virus in naturally-infected cells, primary HTLV-1-infected PBMCs were cultured overnight either under physiologically relevant hypoxia (1% or 2% oxygen) or normoxia (~20% oxygen). RNA was then extracted and subjected to qPCR with primers specific for HTLV-1 *tax* (surrogate for HTLV-1 plus-strand transcription), HTLV-1 *sHBZ* (surrogate for minus-strand HTLV-1 transcription) and host cellular *VEGF* (hypoxia-inducible positive control). There was a significant increase in plus-strand transcription in PBMCs cultured under physiological

hypoxia when compared to PBMCs cultured under ambient oxygen conditions (Figure 1A). No such change was seen in *sHBZ* transcription levels. As expected, there was also a significant upregulation in transcription of the *VEGF* gene, which is regulated by the hypoxia-induced transcription factor (HIF) (Figure 1A).

Epigenetic histone modifications at the HTLV-1 provirus upon reactivation under normoxia and physiological hypoxia

Next, we tested whether the hypoxia-mediated induction of HTLV-1 plus-strand transcription is associated with a specific epigenetic signature in the provirus, by analysing changes in histone methylation status. HTLV-1-infected frozen PBMCs were thawed and either fixed immediately, or cultured overnight under either hypoxia (1% oxygen) or normoxia (20% oxygen) and fixed subsequently at 17 hours. Chromatin from the respective samples was fragmented by sonication and subjected to chromatin immunoprecipitation (ChIP), using antibodies directed against H3K4me3, which is associated with promoters and enhancers; H3K36me3, which is associated with actively-transcribed gene bodies; and H3K27me3, a repressive epigenetic mark associated with heterochromatin.

After overnight incubation, H3K4me3 was observed to be significantly enriched at the 5'-LTR junction, *gag*, *pol*, *env* and *vCTCF* regions of the HTLV-1 provirus in cells cultured in 1% as well as 20% oxygen. By contrast, there was no significant change (within the limits of detection) in H3K4me3 at the 3'-LTR junction (Figure 1B). Similarly, levels of the H3K36me3 mark, which corresponds with proviral activation, were increased across all the regions of the HTLV-1 provirus under physiological hypoxia as well as normoxia (Figure 1C). However, the increase observed in the *gag* and *pol* regions was not statistically significant, perhaps because these regions were highly enriched in the H3K36me3 mark even at time 0 in immediately fixed PBMCs (Figure 1C). Although there was a slight increase in

H3K27me3 levels in all the tested regions of the HTLV-1 provirus upon proviral activation under 1% or 20% oxygen, this increase was statistically significant only in the 3'-LTR junction region (Supplementary figure S1). However, the apparent change in H3K27me3 status was not associated with any perturbation in minus-strand HTLV-1 transcriptional activity in response to hypoxia (Figure 1A), so was not investigated further. H3K4me3 and H3K36me3 are two of the most dynamic histone methylation modifications at the HTLV-1 provirus upon reactivation (M. Miura, AK, unpublished results). However, their levels did not differ within our limits of detection in PBMCs cultured under hypoxia or normoxia.

HTLV-1 plus-strand gene transcription is hypoxia-dependent but Hypoxia Inducible Factor (HIF)-independent

Many transcriptional responses to hypoxia in cells are mediated by the α,β-HIF transcription factors (Kaelin and Ratcliffe, 2008). Under normoxic conditions (oxygen >5%), HIF-1α subunits are efficiently hydroxylated by the HIF prolyl hydroxylases (PHDs) and are rapidly degraded by the ubiquitin-proteasome system. The 3 human PHDs belong to the Fe(II) and 2-oxoglutarate (2-OG)-dependent oxygenase enzyme family, whose activities are dependent on molecular oxygen (O_2). Under hypoxic conditions, PHD activities are inhibited and α,β-HIF is stabilised, so enabling it to orchestrate the cellular response to hypoxia through its role as a transcriptional activator (Figure 2A) (Schofield and Ratcliffe, 2004). Because experimental work under hypoxic conditions imposes significant constraints, hypoxia mimics and HIF stabilisers have been developed to study hypoxia responses under normoxic conditions. Dimethyloxalylglycine (DMOG), a competitive antagonist of 2-OG, is a broad-spectrum inhibitor of 2-OG oxygenases (Figure 2A) (Jaakkola et al., 2001). In contrast, the recently-developed molecule IOX2 is a much more selective inhibitor of the PHDs and stabilises HIF

without affecting the activities of most other 2-OG oxygenases (Figure 2A) (Chowdhury et al., 2013).

We studied the effects of DMOG and IOX2 on the transcriptional activity of the HTLV-1 provirus in PBMCs isolated from infected individuals. The PHD selective inhibitor IOX2 had no effect on HTLV-1 plus-strand transcription (Figure 2B). The PHD inhibition activity of IOX2 in cells was confirmed by a significant increase in transcription of the HIF-1α inducible gene *VEGF* (Figure 2B). Thus the HIF-mediated transcriptional response probably does not play a direct role in the hypoxia-induced increase in HTLV-1 transcription. We observed a small but significant decrease in minus-strand *sHBZ* transcription on treatment with IOX2 (Figure 2B); the reasons for this effect are unknown, but could relate to altered levels of one of the many HIF target genes (which include chromatin-associated proteins (Pollard et al., 2008)). These results imply that HTLV-1 transcription is not directly HIF-regulated, but does involve a hypoxia-related mechanism.

Compared with control cells, DMOG-treated infected PBMCs also showed a significant upregulation in positive control *VEGF* transcription, signifying HIF stabilisation in DMOG-treated cells (Figure 2C) and consistent with the use of DMOG as an experimental mimic of hypoxia (Mole et al., 2003). However, DMOG exerted a strong and paradoxical effect on plus-strand HTLV-1 transcription. In contrast to hypoxia, which induced plus-strand transcription (Figure 1A), DMOG caused a significant and strong inhibition of HTLV-1 plus-strand transcription (Figure 2C). There was also an associated significant increase in minus-strand *sHBZ* transcription after DMOG treatment (Figure 2C). To rule out a possible effect of inhibitor cytotoxicity, dose-response analyses were carried out for both DMOG and IOX2. The results (Supplementary figure S2) confirmed the observations obtained above.

The opposing effects of DMOG on plus- and minus-strand HTLV-1 transcription are independent of each other

The HTLV-1 Tax-mediated positive feedback loop governs plus-strand HTLV-1 transcription. Tax transactivates transcription of the plus-strand genes, including itself. HBZ is encoded by the minus strand and has been reported to inhibit Tax-mediated plus-strand transcription (Basbous et al., 2003; Yoshida et al., 2008). To analyse further the opposing effects of DMOG on plus- and minus-strand HTLV-1 transcription, we investigated the impact of DMOG on HTLV-1 transcription at an earlier time point. After 2 hours of culture of HTLV-1-infected patients' PBMCs with either DMOG or DMSO (control), there was a strong inhibition of *tax* mRNA transcription with DMOG treatment when compared to control (Figure 3). However, there was no corresponding significant increase in *sHBZ* transcription at 2h, suggesting that the inhibitory effect of DMOG on the plus-strand is independent of its effect on the minus-strand (Figure 3). However, a direct or indirect involvement of DMOG on the HBZ protein pools at the 2h time-point cannot be ruled out. Also there was no increase in transcription of the HIF-inducible gene *VEGF* at 2 hours, suggesting that the stabilisation of HIF-1α in response to DMOG treatment did not occur at this early time point (Figure 3) in primary PBMCs.

2-OG oxygenases are not involved in mediating plus-strand HTLV-1 transcription

The 2-OG oxygenase enzyme family plays diverse roles in humans, including roles in collagen biosynthesis, fatty acid metabolism, hypoxic signalling, and nucleic acid and DNA repair and demethylation (Loenarz and Schofield, 2008). We wished to investigate whether specific 2-OG oxygenases regulated the observed epigenetic changes associated with HTLV-1 transcription in primary infected patients' PBMCs. The 2-OG oxygenases with important transcriptional regulatory roles in host cells include the HIF Prolyl Hydroxylases (PHDs), Jumonji C Histone Lysine Demethylases (JmjC KDMs), DNA cytosine hydroxylases (TET

oxygenases) and the AlkB homologue nucleic acid demethylases (Loenarz and Schofield, 2008; Rose et al., 2011), some, but not all, of which are HIF target genes (Pollard et al., 2008).

We had already ruled out the direct involvement of PHDs by employing the selective PHD inhibitor IOX2, which had no effect on plus-strand HTLV-1 transcription (Figure 2B). To further investigate these results, we employed Methylstat (Luo et al., 2011) and JIB-04 (Wang et al., 2013), which are broad-spectrum JumonjiC (JmjC) KDM inhibitors (Supplementary figure S3A). These inhibitors had no significant effects on HTLV-1 plus-strand transcription, consistent with the conclusion that the JmjC KDMs do not play a direct regulatory role in HTLV-1 plus-strand transcription. In agreement with a previous report, Methylstat treatment resulted in a significant reduction in *VEGF* mRNA transcription (Cho et al., 2014). In contrast, JIB-04 treatment significantly induced *VEGF* transcription (Supplementary figure S3A). To our knowledge, there have been no prior studies examining the effect of JIB-04 on *VEGF* mRNA and angiogenesis. Furthermore, ChIP analysis showed no significant difference in either H3K4me3 or H3K36me3 when compared to control (DMSO) in the 5′-LTR and the *gag* region of the provirus (Supplementary figure S3 B and C). There was a significant increase in H3K4me3 at the 3'-LTR in DMOG-treated samples, compared with control (Supplementary figure S3B). This increase is consistent with the observed increase in *sHBZ* mRNA levels following DMOG treatment (Figure 2C). There was no difference in the DNA methylation profile between DMOG-treated and DMSO (control)-treated samples (Supplementary figure S3D), indicating that members of the TET and (at least some of the) AlkB homologue subfamilies of DNA demethylases/hydroxylases (nucleic acid oxygenases) are unlikely to be directly involved in regulating the observed spontaneous HTLV-1 plus-strand transcription. We conclude that the epigenetic effector 2-OG oxygenases are not directly involved in HTLV-1 plus-strand transcription (within our limits of detection).

Metabolic effects of DMOG on PBMCs from HTLV-1 infected individuals

2-Oxoglutarate (2-OG, or alpha-ketoglutarate), in addition to being a co-susbtrate for 2-OG oxygenases, is also an important intermediate in metabolism, specifically the TCA cycle, oxidative phosphorylation, and amino acid metabolism. To test the hypothesis that DMOG influences HTLV-1 transactivation through perturbation of these cellular metabolic pathways (in a HIF independent manner), we treated HTLV-1-infected patients' PBMCs overnight with either 0.5 mM DMOG in DMSO, or DMSO alone (control). The cells were lysed and the extracts subjected to ion-exchange liquid chromatography coupled directly to tandem mass spectrometry (MS/MS), to identify the metabolic pathways modulated by DMOG. Untargeted metabolite profiling measured 4261 molecular species with a unique mass-to-charge ratio. The identified metabolites (N = 137) were sorted according to the maximum fold-change in the normalized abundance between DMSO-treated and DMOG-treated samples respectively. Any change that was statistically significant ($p<0.05$) and exceeded 1.3-fold was analysed further (raw data with identified metabolites provided in Supplementary file S2). N-Oxalylglycine (NOG) was found in high abundance in DMOG treated cells, but not DMSO controls (Supplementary file S2). This observation is commensurate with hydrolysis of the pro-drug DMOG to NOG in cells by carboxylesterases (Zhdanov et al., 2015). Endogenous metabolites that showed a statistically significant difference were sorted according to the metabolic pathways in which they participate.

The results showed significant changes in six metabolic pathways:

(i) Glycolysis. A significant reduction was observed in the levels of most of the measured glycolytic intermediates in response to DMOG treatment. In particular, intermediates towards the end of glycolysis: 2, 3-diphosphoglycerate and 3-phosphoglycerate were highly depleted in DMOG-treated cells (Figure 4). Glyceraldehyde-3-phosphate and alpha-D-glucose 6-

phosphate were the only glycolytic intermediates that showed significantly higher levels in DMOG-treated cells compared to control (Figure 4). Pyruvate levels remained largely unchanged in response to DMOG treatment (Supplementary file S2). There was a significant reduction in the level of glycolysis and TCA cycle products NADH and ATP in response to DMOG treatment.

(ii) TCA Cycle. Being an analogue of the TCA cycle metabolite 2-OG, DMOG affects the TCA cycle (Rendina et al., 2013); Specifically, the levels of the TCA cycle intermediates citrate, cis-aconitate, isocitrate, 2-OG and malate were significantly lower in DMOG-treated HTLV-1 infected PBMCs than in control (DMSO-treated) cells. Only succinate levels remained unchanged, among the measured TCA cycle metabolites, in response to DMOG treatment. DMOG inhibits mitochondrial respiration independently of its hypoxia mimic effect (Zhdanov et al., 2015).

(iii) Pentose phosphate pathway. Higher levels of glyceraldehyde-3-phosphate, alpha-D-glucose 6-phosphate, 6-phosphogluconate, ribulose 5-phosphate and D-ribose in combination with low levels of 1-deoxy-D-xylulose 5-phosphate, deoxyribose 5-phosphate and sedoheptulose 1,7-bisphosphate in DMOG-treated samples when compared to control pointed towards a downstream inhibition in the pentose phosphate pathway in response to DMOG treatment.

(iv) Redox metabolism. The pentose phosphate pathway is responsible for synthesis of NADPH, a reducing equivalent in cell metabolism (Stincone et al., 2015), e.g. in the conversion of oxidized glutathione disulphide (GSSG) to reduced glutathione (GSH) for counteracting cellular redox stress. The decrease in cellular NADPH levels, together with the associated decrease in glutathione levels in DMOG-treated cells, suggests that the DMOG-treated cells were under oxidative stress. This proposal is supported by the observed impairment (in response to DMOG) in oxidative phosphorylation (ii above) and the

mitochondrial electron transport chain, both of which generate oxidative stress (Cadenas and Davies, 2000; Rendina et al., 2013).

(v) Purine and pyrimidine metabolism. While levels of purine metabolites adenosine and guanosine monophosphate (AMP and GMP) were significantly higher in DMOG-treated cells when compared to controls, the corresponding nucleoside triphosphates (ATP and GTP) were significantly depleted. All pyrimidine metabolites measured (UTP, UMP, CTP and CMP) were depleted in DMOG-treated cells when compared to control. dCTP, a precursor for DNA synthesis, was strongly inhibited by DMOG treatment.

(vi) Amino acid, carbohydrate and lipid metabolism. DMOG treatment resulted in a significant increase in L-tryptophan levels. This might be expected given the strong concomitant reduction in tryptophan degradation products, quinolinic acid and 2-aminomuconic acid semialdehyde, observed in the DMOG-treated samples. Inhibition of glucose metabolism by DMOG might in turn inhibit many anabolic processes, because of the reduction in ATP and NADH. The observed significant decrease in the levels of N-acetylated metabolites could be due to the limited availability of acetyl CoA resulting from an inhibition of glycolysis and the TCA cycle.

Thus most of the observed metabolic effects of DMOG, discussed above, are secondary to its perturbation of glycolysis, the TCA cycle and oxidative phosphorylation (Figure 4). Hence we went on to target these pathways with specific inhibitors to study if selective inhibition of certain enzymes could inhibit *tax* transcription in HTLV-1-infected primary PBMCs.

The rate of glycolysis, but not the concentrations of TCA cycle intermediates, is linked to plus-strand HTLV-1 transcription

To investigate the influence of glucose metabolism on HTLV-1 transcription, we tested the effects of the TCA cycle inhibitor sodium arsenite (Bergquist et al., 2009) and the glycolysis

inhibitor iodoacetate (IAA) (Sabri and Ochs, 1971)(Figure 5A) and quantified their effects on HTLV-1 plus-strand transcription in primary PBMCs derived from HTLV-1-infected individuals.

IAA treatment significantly inhibited HTLV-1 *tax* mRNA transcription, whereas arsenite caused no change in *tax* mRNA levels at the concentration tested (Figure 5A). The stress-inducible enzyme heme oxygenase 1 (HMOX1) served as the positive control for the biological activity of the drugs (Figure 5A). IAA and arsenite also inhibited cellular *VEGF* mRNA levels (Figure 5A). These results suggest that glucose metabolism influences reactivation of HTLV-1 from latency and reinforce the conclusion that HTLV-1 *tax* mRNA transcription is independent of HIF and intracellular oxidative stress. Neither IAA nor arsenite made an impact on minus-strand HTLV-1 transcription (Supplementary figure S4A).

As a further test of the involvement of glucose metabolism in HTLV-1 transactivation from latency, primary PBMCs from HTLV-1-infected individuals were cultured in RPMI medium with either 5.5 mM glucose with 10% FBS (physiological glucose concentrations) or 0 mM glucose with 10% FBS in the presence or absence of the glycolysis inhibitor 2-deoxy-D-glucose (2-DG) (Zhong et al., 2009) and the TCA cycle inducers sodium pyruvate (Diers et al., 2012) or galactose (Aguer et al., 2011) (Figure 5B).

PBMCs from HTLV-1-infected individuals cultured overnight in RPMI with 0 mM glucose + 10% FBS expressed significantly lower levels of HTLV-1 *tax* mRNA than did PBMCs cultured in RPMI with physiological (5.5 mM) glucose + 10% FBS. Addition of the glycolysis inhibitor 2-DG to the 0 mM glucose medium led to a further significant suppression of HTLV-1 plus-strand transcription. Further addition of the TCA cycle inducer sodium pyruvate (0 mM glucose + 2-DG + pyruvate) did not rescue the inhibitory effect of 2-

DG on HTLV-1 *tax* transcription. These observations are consistent with the data shown in Figure 5A; they indicate that glycolysis, but not the TCA cycle, plays an important role in HTLV-1 plus-strand transcription. Galactose, an inducer of the TCA cycle and oxidative phosphorylation, had no effect on HTLV-1 plus-strand transcription when added to 0 mM glucose medium, strengthening the conclusion that the TCA cycle is not involved in HTLV-1 reactivation from latency. Like IAA and arsenite, 2-DG treatment also resulted in a significant reduction in cellular *VEGF* mRNA levels. Inhibition of glycolysis by 2-DG also resulted in a significant decrease in the mRNA of lactate dehydrogenase A, a surrogate marker of the rate of glycolysis (Figure 5B). There was no significant difference in *sHBZ* transcription upon either inhibition of glycolysis (by incubation in 0 mM Glucose or 2-DG) or TCA cycle induction (by pyruvate or galactose) when compared to control (Supplementary figure S4B).

Inhibition of the mitochondrial electron transport chain (ETC) inhibits plus-strand HTLV-1 transcription

Next, we studied the effect of inhibition of the mitochondrial ETC on HTLV-1 plus-strand transcription. PBMCs from HTLV-1-infected individuals were incubated overnight in the presence or absence of inhibitors of mitochondrial ETC complex II (3-nitropropionic acid (3-NPA): Figure 6A), complex I (rotenone: Figure 6B), complex III (antimycin A and myxothiazol: Figure 6B) and complex V (oligomycin: Figure 6B) (Rohlena et al., 2013).

Four out of five mitochondrial ETC complex inhibitors tested caused a significant reduction in plus-strand HTLV-1 transcription (Figure 6A and 6B): only oligomycin, an inhibitor of complex V, had no impact on HTLV-1 *tax* transcription (Figure 6B). These inhibitors had varying effects on *VEGF* and *LDHA* mRNA levels (Figure 6A and 6B). Also, there was no change in minus-strand *sHBZ* transcription in response to ETC inhibitor treatment

(Supplementary figure S4C). These results suggest that the mode of action of the ETC inhibitors on plus-strand HTLV-1 transcription is an independent phenomenon and is not mediated through their perturbation of the glycolytic and hypoxia pathways in cells.

Discussion

$CD4^+$ T-lymphocytes, the primary reservoir of HTLV-1 in humans, are routinely exposed in vivo to alterations in the microenvironment such as changes in the oxygen tension or the concentration of glucose and other nutrients. We hypothesised that such changes influence the transcriptional activity of the HTLV-1 provirus, which is usually silent in freshly isolated PBMCs but undergoes strong spontaneous activation ex vivo. To minimize artefacts due to in vitro selection, we studied fresh PBMCs isolated from HTLV-1-infected individuals.

HTLV-1-infected primary PBMCs cultured under conditions of physiological hypoxia (1% or 2% oxygen) showed a significant enhancement in HTLV-1 plus-strand transcription when compared to those cultured under ambient oxygen conditions (~20% oxygen) (Figure 1). Hypoxia has been shown to have variable effects on viral expression within cells. For example, hypoxia induces lytic replication in human herpesvirus-8 (HHV-8) (Davis et al., 2001), whereas Tat-induced HIV-1 transcription is inhibited by hypoxia (Charles et al., 2009). Thus, viruses have developed different adaptive responses to varying oxygen levels within the body. By employing a specific HIF-stabiliser IOX2 (Chowdhury et al., 2013), we showed that the hypoxia-mediated effect on HTLV-1 transcription appeared to be independent of HIF (Figure 2B). The effect of physiological hypoxia on HTLV-1 transcription suggests that the dynamics of HTLV-1 reactivation that we observe in freshly isolated PBMCs from venous blood differ from the dynamics in other compartments such as solid lymphoid tissue or bone marrow, where the oxygen tension is typically 1% to 2%

(Ivanovic, 2009; Ohta et al., 2011). Since hypoxia enhances plus-strand proviral transcription, the infected cells in these compartments might be more likely to support productive viral replication and spread. Consistent with this hypothesis, Yasunaga et al reported higher levels of *tax* mRNA in the bone marrow than in other tissues (Yasunaga et al., 2016).

In contrast to the effect of hypoxia, the hypoxia mimic DMOG potently inhibited proviral plus-strand transcription in HTLV-1-infected primary PBMCs (Figure 2C). We therefore investigated the HIF-independent effects of DMOG, either as an inhibitor of 2-OG oxygenases or as an inhibitor of glucose metabolism and the TCA cycle. Having ruled out the involvement of epigenetic effector 2-OG oxygenases including PHDs (Figure 2B, C), JmjC lysine demethylases (Supplementary figure S3A, B and C) and nucleic acid oxygenases (Supplementary figure S3D), we studied the influence of glucose metabolism on HTLV-1 transcription. Mass spectrometry of DMOG-treated HTLV-1-infected primary PBMCs revealed that DMOG significantly inhibited all the metabolic pathways closely linked to glucose metabolism (Figure 4). It is known that DMOG inhibits TCA cycle and mitochondrial respiration (Rendina et al., 2013; Zhdanov et al., 2015) but direct inhibition of glycolysis by DMOG has not previously been reported.

Chemical inhibition of glycolysis by either iodoacetic acid or 2-DG significantly reduced plus-strand HTLV-1 transcription (Figure 5). However, neither an inhibitor (arsenite) nor inducers (sodium pyruvate and galactose) of the TCA cycle altered HTLV-1 transcription. We conclude that glycolysis regulates reactivation from latency of the integrated HTLV-1 provirus. Consistent with this effect, we saw a significant reduction in HTLV-1 plus-strand transcription in PBMCs cultured in glucose-free medium when compared to those cultured under physiological glucose concentration (5.5mM). The glucose receptor GLUT-1 is a

cellular receptor for HTLV-1 infection (Manel et al., 2003); expression of GLUT-1 is induced by hypoxia and other forms of cellular stress.

Four out of five inhibitors of the mitochondrial electron transport chain tested significantly reduced HTLV-1 transcription (Figure 6). Specifically, inhibitors of ETC complexes involved in electron transfer (Complex I, II and III) reduced HTLV-1 plus-strand transcription. However, inhibition of mitochondrial ATP synthase (Complex V) by oligomycin had no impact (Figure 6). It is unclear why oligomycin had no effect on HTLV-1 transcription at the tested concentration. The ETC inhibitors had variable effects on expression of the hypoxia-inducible gene *VEGF* and the glycolytic enzyme *LDHA*, suggesting that their effect on HTLV-1 transcription is independent of hypoxia and glycolysis. Ciminale and colleagues have shown that the p13 accessory protein of HTLV-1 modulates mitochondrial membrane potential by facilitating an inward K^+ current, thereby increasing ETC activity and ROS production, consistent with a link between mitochondrial function and the HTLV-1 life cycle (Silic-Benussi et al., 2010; Silic-Benussi et al., 2009).

We propose that the strong inhibition of HTLV-1 caused by DMOG is due to inhibition of both glycolysis and the mitochondrial ETC. Thus, glycolysis and the mitochondrial ETC play an important role in regulating HTLV-1 plus-strand transcription, whereas the TCA cycle does not play a direct role. In the light of the recent observations that different subsets of T-cells rely on different metabolic pathways for their energy needs (Buck et al., 2015; Dimeloe et al., 2017), it is plausible that the TCA cycle contributes less than glycolysis to the metabolism of HTLV-1-infected $CD4^+$ T-cells.

A typical HTLV-1-infected individual has approximately 10^4 to 10^5 different HTLV-1-infected T-cell clones, each with a unique proviral integration site (Gillet et al., 2011; Laydon

et al., 2014; Melamed et al., 2013). We conclude that both viral determinants (e.g. genomic integration site, orientation) and the host microenvironment (e.g. glucose concentration, oxygen levels) determine the likelihood of spontaneous reactivation of an integrated HTLV-1 provirus from a latent state.

Significance

Retroviruses such as HTLV-1 persist life-long in their host by integrating a copy of their genetic material into the host cellular genomic DNA. Although HTLV-1 infection is asymptomatic in most cases, in a subset of infected individuals (~10%) it causes an aggressive haematological malignancy or a debilitating neuro-inflammatory condition. Infection is considered largely latent due to the absence of viral RNA and proteins in fresh blood samples. However, when blood obtained from HTLV-1 infected individuals is cultured ex vivo, there is a spontaneous increase in plus-strand HTLV-1 transcription, which suggests that changes in the extracellular microenvironment play an important deterministic role in viral expression. Here, we identify two factors in the microenvironment that regulate HTLV-1 proviral latency and expression. First, we show that physiological hypoxia (1% or 2% oxygen), as present in the lymphoid organs and bone marrow, enhances HTLV-1 transcription. Second, inhibition of glycolysis or the mitochondrial electron transport chain suppresses plus-strand HTLV-1 transcription. We conclude that both glucose metabolism and oxygen availability regulate HTLV-1 transcription. The significance of these results is twofold. First, the identification of two microenvironmental factors that regulate HTLV-1 expression constitutes a basic advance in the understanding of HTLV-1 persistence and pathogenesis. Second, targeting these pathways with currently available as well as novel therapies could complement existing antiretrovirals and improve treatment efficiency.

Supplemental information

Supplemental information includes four figures (Figures S1 – S4), two tables (Tables S1 and S2) and two supplementary excel files (Files S1 and S2).

Author contributions

Conceived and designed the experiments: AK, CCT, CJS, CRMB; Performed the experiments: AK, MM, JSM; Analyzed the data: AK, JSM, CJS, CRMB; Contributed reagents/materials/analysis tools: CCT, CJS, JSM; Writing-original draft: AK, CRMB; Writing-review and editing: AK, CRMB, CJS, JSM, GPT; Recruited patients: GPT.

Acknowledgements

We thank Norma Masson, David Mole, Peter Ratcliffe, Akane Kawamura and members of the CRMB and CJS laboratories for helpful discussions. This work was supported by a Project Grant from the Medical Research Council, U.K. (MR/K019090/1) and Senior Investigator Award from the Wellcome Trust, U.K. (WT100291MA) to CRMB.

Bibliography

Aguer, C., Gambarotta, D., Mailloux, R.J., Moffat, C., Dent, R., McPherson, R., and Harper, M.E. (2011). Galactose enhances oxidative metabolism and reveals mitochondrial dysfunction in human primary muscle cells. PLoS One 6, e28536.

Bangham, C.R.M. (2009). CTL quality and the control of human retroviral infections. Eur J Immunol 39, 1700-1712.

Basbous, J., Arpin, C., Gaudray, G., Piechaczyk, M., Devaux, C., and Mesnard, J.M. (2003). The HBZ factor of human T-cell leukemia virus type I dimerizes with transcription factors JunB and c-Jun and modulates their transcriptional activity. J Biol Chem 278, 43620-43627.

Bergquist, E.R., Fischer, R.J., Sugden, K.D., and Martin, B.D. (2009). Inhibition by methylated organo-arsenicals of the respiratory 2-oxo-acid dehydrogenases. J Organomet Chem 694, 973-980.

Buck, M.D., O'Sullivan, D., and Pearce, E.L. (2015). T cell metabolism drives immunity. J Exp Med 212, 1345-1360.

Cadenas, E., and Davies, K.J. (2000). Mitochondrial free radical generation, oxidative stress, and aging. Free Radic Biol Med 29, 222-230.

Charles, S., Ammosova, T., Cardenas, J., Foster, A., Rotimi, J., Jerebtsova, M., Ayodeji, A.A., Niu, X., Ray, P.E., Gordeuk, V.R., et al. (2009). Regulation of HIV-1 transcription at 3% versus 21% oxygen concentration. J Cell Physiol 221, 469-479.

Cho, Y., Kim, K.H., Cho, Y.S., Xu, W.Q., Wang, X., and Kwon, H.J. (2014). A histone demethylase inhibitor, methylstat, inhibits angiogenesis in vitro and in vivo. Rsc Advances 4, 38230-38233.

Chowdhury, R., Candela-Lena, J.I., Chan, M.C., Greenald, D.J., Yeoh, K.K., Tian, Y.M., McDonough, M.A., Tumber, A., Rose, N.R., Conejo-Garcia, A., et al. (2013). Selective small molecule probes for the hypoxia inducible factor (HIF) prolyl hydroxylases. ACS Chem Biol 8, 1488-1496.

Cikos, S., Bukovska, A., and Koppel, J. (2007). Relative quantification of mRNA: comparison of methods currently used for real-time PCR data analysis. BMC Mol Biol 8, 113.

Davis, D.A., Rinderknecht, A.S., Zoeteweij, J.P., Aoki, Y., Read-Connole, E.L., Tosato, G., Blauvelt, A., and Yarchoan, R. (2001). Hypoxia induces lytic replication of Kaposi sarcoma-associated herpesvirus. Blood 97, 3244-3250.

Diers, A.R., Broniowska, K.A., Chang, C.F., and Hogg, N. (2012). Pyruvate fuels mitochondrial respiration and proliferation of breast cancer cells: effect of monocarboxylate transporter inhibition. Biochem J 444, 561-571.

Dimeloe, S., Burgener, A.V., Grahlert, J., and Hess, C. (2017). T-cell metabolism governing activation, proliferation and differentiation; a modular view. Immunology 150, 35-44.

Ebbesen, P., and Zachar, V. (1998). Oxygen tension and virus replication. Acta Virol 42, 417-421.

Gillet, N.A., Malani, N., Melamed, A., Gormley, N., Carter, R., Bentley, D., Berry, C., Bushman, F.D., Taylor, G.P., and Bangham, C.R. (2011). The host genomic environment of the provirus determines the abundance of HTLV-1-infected T-cell clones. Blood 117, 3113-3122.

Hangai-Hoger, N., Tsai, A.G., Cabrales, P., and Intaglietta, M. (2007). Terminal lymphatics: the potential "lethal corner" in the distribution of tissue pO2. Lymphat Res Biol 5, 159-168.

Hanon, E., Hall, S., Taylor, G.P., Saito, M., Davis, R., Tanaka, Y., Usuku, K., Osame, M., Weber, J.N., and Bangham, C.R. (2000). Abundant tax protein expression in CD4+ T cells infected with human T-cell lymphotropic virus type I (HTLV-I) is prevented by cytotoxic T lymphocytes. Blood 95, 1386-1392.

Ivanovic, Z. (2009). Hypoxia or in situ normoxia: The stem cell paradigm. J Cell Physiol 219, 271-275.

Jaakkola, P., Mole, D.R., Tian, Y.M., Wilson, M.I., Gielbert, J., Gaskell, S.J., von Kriegsheim, A., Hebestreit, H.F., Mukherji, M., Schofield, C.J., et al. (2001). Targeting of HIF-alpha to the von Hippel-Lindau ubiquitylation complex by O2-regulated prolyl hydroxylation. Science 292, 468-472.

Kaelin, W.G., Jr., and Ratcliffe, P.J. (2008). Oxygen sensing by metazoans: the central role of the HIF hydroxylase pathway. Mol Cell 30, 393-402.

Laydon, D.J., Melamed, A., Sim, A., Gillet, N.A., Sim, K., Darko, S., Kroll, J.S., Douek, D.C., Price, D.A., Bangham, C.R., et al. (2014). Quantification of HTLV-1 clonality and TCR diversity. PLoS Comput Biol 10, e1003646.

Loenarz, C., and Schofield, C.J. (2008). Expanding chemical biology of 2-oxoglutarate oxygenases. Nature Chemical Biology 4, 152-156.

Luo, X., Liu, Y., Kubicek, S., Myllyharju, J., Tumber, A., Ng, S., Che, K.H., Podoll, J., Heightman, T.D., Oppermann, U., et al. (2011). A selective inhibitor and probe of the cellular functions of Jumonji C domain-containing histone demethylases. J Am Chem Soc 133, 9451-9456.

Manel, N., Kim, F.J., Kinet, S., Taylor, N., Sitbon, M., and Battini, J.L. (2003). The ubiquitous glucose transporter GLUT-1 is a receptor for HTLV. Cell 115, 449-459.

Melamed, A., Laydon, D.J., Gillet, N.A., Tanaka, Y., Taylor, G.P., and Bangham, C.R. (2013). Genome-wide determinants of proviral targeting, clonal abundance and expression in natural HTLV-1 infection. PLoS Pathog 9, e1003271.

Mohyeldin, A., Garzon-Muvdi, T., and Quinones-Hinojosa, A. (2010). Oxygen in stem cell biology: a critical component of the stem cell niche. Cell Stem Cell 7, 150-161.

Mole, D.R., Schlemminger, I., McNeill, L.A., Hewitson, K.S., Pugh, C.W., Ratcliffe, P.J., and Schofield, C.J. (2003). 2-oxoglutarate analogue inhibitors of HIF prolyl hydroxylase. Bioorg Med Chem Lett 13, 2677-2680.

Morinet, F., Casetti, L., Francois, J.H., Capron, C., and Pillet, S. (2013). Oxygen tension level and human viral infections. Virology 444, 31-36.

Ohta, A., Diwanji, R., Kini, R., Subramanian, M., Ohta, A., and Sitkovsky, M. (2011). In vivo T cell activation in lymphoid tissues is inhibited in the oxygen-poor microenvironment. Front Immunol 2, 27.

Pollard, P.J., Loenarz, C., Mole, D.R., McDonough, M.A., Gleadle, J.M., Schofield, C.J., and Ratcliffe, P.J. (2008). Regulation of Jumonji-domain-containing histone demethylases by hypoxia-inducible factor (HIF)-1alpha. Biochem J 416, 387-394.

Rende, F., Cavallari, I., Corradin, A., Silic-Benussi, M., Toulza, F., Toffolo, G.M., Tanaka, Y., Jacobson, S., Taylor, G.P., D'Agostino, D.M., et al. (2011). Kinetics and intracellular compartmentalization of HTLV-1 gene expression: nuclear retention of HBZ mRNAs. Blood 117, 4855-4859.

Rendina, A.R., Pietrak, B., Smallwood, A., Zhao, H., Qi, H., Quinn, C., Adams, N.D., Concha, N., Duraiswami, C., Thrall, S.H., et al. (2013). Mutant IDH1 enhances the production of 2-hydroxyglutarate due to its kinetic mechanism. Biochemistry 52, 4563-4577.

Rohlena, J., Dong, L.F., and Neuzil, J. (2013). Targeting the mitochondrial electron transport chain complexes for the induction of apoptosis and cancer treatment. Curr Pharm Biotechnol 14, 377-389.

Rose, N.R., McDonough, M.A., King, O.N., Kawamura, A., and Schofield, C.J. (2011). Inhibition of 2-oxoglutarate dependent oxygenases. Chem Soc Rev 40, 4364-4397.

Sabri, M.I., and Ochs, S. (1971). Inhibition of glyceraldehyde-3-phosphate dehydrogenase in mammalian nerve by iodoacetic acid. J Neurochem 18, 1509-1514.

Satou, Y., Miyazato, P., Ishihara, K., Yaguchi, H., Melamed, A., Miura, M., Fukuda, A., Nosaka, K., Watanabe, T., Rowan, A.G., et al. (2016). The retrovirus HTLV-1 inserts an ectopic CTCF-binding site into the human genome. Proc Natl Acad Sci U S A 113, 3054-3059.

Schofield, C.J., and Ratcliffe, P.J. (2004). Oxygen sensing by HIF hydroxylases. Nat Rev Mol Cell Biol 5, 343-354.

Silic-Benussi, M., Biasiotto, R., Andresen, V., Franchini, G., D'Agostino, D.M., and Ciminale, V. (2010). HTLV-1 p13, a small protein with a busy agenda. Mol Aspects Med 31, 350-358.

Silic-Benussi, M., Cannizzaro, E., Venerando, A., Cavallari, I., Petronilli, V., La Rocca, N., Marin, O., Chieco-Bianchi, L., Di Lisa, F., D'Agostino, D.M., et al. (2009). Modulation of mitochondrial K(+) permeability and reactive oxygen species production by the p13 protein of human T-cell leukemia virus type 1. Biochim Biophys Acta 1787, 947-954.

Stincone, A., Prigione, A., Cramer, T., Wamelink, M.M., Campbell, K., Cheung, E., Olin-Sandoval, V., Gruning, N.M., Kruger, A., Tauqeer Alam, M., et al. (2015). The return of metabolism: biochemistry and physiology of the pentose phosphate pathway. Biol Rev Camb Philos Soc 90, 927-963.

Tsai, A.G., Cabrales, P., Hangai-Hoger, N., and Intaglietta, M. (2004). Oxygen distribution and respiration by the microcirculation. Antioxid Redox Signal 6, 1011-1018.

Wang, L., Chang, J., Varghese, D., Dellinger, M., Kumar, S., Best, A.M., Ruiz, J., Bruick, R., Pena-Llopis, S., Xu, J., et al. (2013). A small molecule modulates Jumonji histone demethylase activity and selectively inhibits cancer growth. Nat Commun 4, 2035.

Yasunaga, J.-i., Furuta, R., Miura, M., Sugata, K., Saito, A., Hirofumi, A., Ueno, T., Takenouchi, N., Fujisawa, J.-i., Shimizu, M., et al. (2016). Hematopoietic Stem Cell Infected with HTLV-1 Functions As a Viral Reservoir In Vivo. Blood 128, 1343-1343.

Yoshida, M., Satou, Y., Yasunaga, J., Fujisawa, J., and Matsuoka, M. (2008). Transcriptional control of spliced and unspliced human T-cell leukemia virus type 1 bZIP factor (HBZ) gene. J Virol 82, 9359-9368.

Zhdanov, A.V., Okkelman, I.A., Collins, F.W.J., Melgar, S., and Papkovsky, D.B. (2015). A novel effect of DMOG on cell metabolism: direct inhibition of mitochondrial function precedes HIF target gene expression. Biochimica Et Biophysica Acta-Bioenergetics 1847, 1254-1266.

Zhong, D., Xiong, L., Liu, T., Liu, X., Liu, X., Chen, J., Sun, S.Y., Khuri, F.R., Zong, Y., Zhou, Q., et al. (2009). The glycolytic inhibitor 2-deoxyglucose activates multiple prosurvival pathways through IGF1R. J Biol Chem 284, 23225-23233.

Figure legends

Figure 1: (A) Hypoxia enhances plus-strand HTLV-1 (*tax*) transcription. PBMCs isolated from HTLV-1-infected individuals (n=11) were cultured overnight either under atmospheric oxygen conditions (20% oxygen) or under hypoxia (1% or 2% oxygen). RNA was extracted and subjected to RT-qPCR with primers specific for *tax* mRNA (plus-strand), *sHBZ* mRNA (minus-strand) or *VEGF* mRNA (positive control). Error bars represent the standard error of the mean. Statistical significance was calculated using the two-tailed Student's T-test where ** represents $p<0.005$ and ns represents not significant. **(B, C) Epigenetic changes at the HTLV-1 provirus upon reactivation under physiological hypoxia or normoxia.** HTLV-1-infected PBMCs were either fixed immediately (T_0) or cultured overnight under hypoxia (1% oxygen) or normoxia (20% oxygen) and subsequently fixed and subjected to ChIP-qPCR, using antibodies directed against H3K4me3, H3K36me3 and IgG and primers specific for the 5'-LTR Jn, *Gag*, *Pol*, *Env*, *vCTCF*, *Tax* and 3'-LTR Jn of the HTLV-1 LTR. Enrichment is expressed as % input DNA and normalized to T0 at the 5'-LTR junction. Error bars represent the standard error of 4 independent ChIP experiments. Statistical significance was calculated using the two-tailed Student's T-test where * represents $p<0.05$, ** represents $p<0.005$.

Figure 2: (A) Specificity of the two hypoxia mimics employed. IOX2 is a selective PHD inhibitor while DMOG is a competitive antagonist of 2-oxoglutarate (2-OG) binding which acts as broad-spectrum inhibitor of 2OG-dependent oxygenases. **(B, C)** Evidence that **HTLV-1 transcription is hypoxia-dependent, but HIF-independent.** PBMCs isolated from HTLV-1-infected individuals were incubated overnight in the presence or absence of either IOX2 (B) or DMOG (C). RNA was extracted and subjected to RT-qPCR with primers

specific for *tax* mRNA (plus-strand), *sHBZ* mRNA (minus-strand) or *VEGF* mRNA (positive control). Error bars represent the standard error of samples treated respectively with IOX2 (n = 7) and DMOG (n = 11). Statistical significance was calculated using the two-tailed Student's T-test where * represents $p<0.05$, ** represents $p<0.005$ and *** represents $p<0.0005$.

Figure 3: The effect of DMOG on plus-strand HTLV-1 transcription is independent of its effect on the minus-strand. HTLV-1-infected primary PBMCs were treated for 2 hours with either DMOG or DMSO (control). RNA was extracted and subjected to RT-qPCR with primers specific for *tax* mRNA (plus-strand), *sHBZ* mRNA (minus-strand) or *VEGF* mRNA (positive control). Error bars represent the standard error of the mean (n = 5). Statistical significance was calculated using the two-tailed Student's T-test where *** represents $p<0.0005$.

Figure 4: Metabolomic (LC-MS/MS) analysis of DMOG-treated HTLV-1-infected cells. Primary PBMCs from HTLV-1-infected subjects (n = 5) were treated with either 0.5mM DMOG or DMSO (control) overnight. Cells were lysed and subjected to metabolomic analysis by mass spectrometry as mentioned in the methods section. The blue bars depict significant ($p<0.05$) fold changes in the abundance of identified metabolites in response to DMOG treatment when compared to control samples. The bars on the right of the Y-axis correspond to metabolites induced by DMOG treatment while those on the left correspond to metabolites depleted after DMOG treatment. The metabolites have been grouped according to their respective metabolic pathways. The shaded area corresponds to a fold-change from -1 to 1 (no change in metabolite levels in response to DMOG treatment).

Figure 5: The rate of glycolysis, but not the TCA cycle, is intimately linked to plus-strand HTLV-1 transcription. HTLV-1-infected primary PBMCs were treated overnight with either control (water), iodoacetic acid (IAA) or sodium arsenite **(panel A)** or cultured under indicated concentrations of glucose-containing RPMI in the presence or absence of the glycolysis inhibitor 2-deoxy-D-glucose (2-DG) & TCA cycle inducers sodium pyruvate and galactose **(panel B)**. RNA was extracted and subjected to RT-qPCR with primers specific for *tax* mRNA (plus-strand), heme oxygenase 1 (*HMOX1)* mRNA (positive control for IAA and arsenite), *VEGF* mRNA and lactate dehydrogenase A (*LDHA)* mRNA (indicator for rate of glycolysis). Error bars represent standard error of the mean (N=8), except for HMOX1 in panel (A) where n = 4. Statistical significance was calculated using the two-tailed Student's T-test where *** represents $p<0.0005$, ** represents $p<0.005$ and * represents $p<0.05$.

Figure 6: Inhibition of the mitochondrial electron transport chain (ETC) inhibits plus-strand HTLV-1 transcription. HTLV-1 infected primary PBMCs were cultured overnight in the presence of the indicated compounds. RNA was extracted and subjected to RT-qPCR with primers specific for *tax* mRNA (plus-strand), *VEGF* mRNA and *LDHA* mRNA. Error bars represent the standard error of the mean (n = 8). Statistical significance was calculated by the paired Wilcoxon signed rank test where ** represents $p<0.005$ and * represents $p<0.05$.

STAR ★METHODS

CONTACT FOR REAGENT AND RESOURCE SHARING

Further information and requests for reagents may be directed to, and will be fulfilled by, the corresponding author Charles R.M. Bangham (c.bangham@imperial.ac.uk)

EXPERIMENTAL MODEL DETAILS

Human specimens

A list of patient blood samples tested has been provided in Supplementary file S1. All donors attended the National Centre for Human Retrovirology (NCHR) at Imperial College Healthcare NHS Trust, St Mary's Hospital, London and gave written informed consent in accordance with the Declaration of Helsinki to donate blood samples to the Communicable Diseases Research Tissue Bank which is approved by the UK National Research Ethics Service (15/SC/0089).

METHOD DETAILS

Primary T-cell isolation and culture

Venous blood samples from HTLV-1-infected individuals attending the NCHR HTLV clinic were separated using Histopaque and PBMCs stored in liquid nitrogen. CD8+ T-cells were depleted from PBMCs with Dynabeads CD8 (ThermoFisher Scientific), using the manufacturer's instructions. Equal volumes of RPMI with L-Glutamine without Glucose (BE12-752F, Lonza) and RPMI with L-Glutamine and 11mM Glucose (BE12-702F) were mixed to make RPMI with L-Glutamine and 5.5mM Glucose. This medium was used for cell culture with 10% FBS (Gibco) in all experiments, unless otherwise stated.

Hypoxia culture

A 'Hypoxylab' (Oxford Optronix, Oxford, UK) - hypoxia workstation and incubator was employed for all hypoxia-related experiments. All media and consumables used in hypoxic

culture were conditioned to the target oxygen concentration (1% or 2%) before use. Primary PBMCs were manipulated and cultured in the HypoxyLab at the desired oxygen concentration for the indicated time. In situ dissolved oxygen in the culture media was measured using the integrated OxyLite™ (Oxford Optronix) oxygen sensor to accurately monitor oxygen availability in the cellular microenvironment.

Inhibitors

Multiple chemical inhibitors of different cellular pathways were employed in this study. A comprehensive list of all the compounds used along with the corresponding references is provided in Supplementary table S1. Stocks of each inhibitor were prepared in either DMSO or water, and diluted to their desired concentration in culture medium to study their effects on HTLV-1 transcription.

RNA extraction and qRT-PCR

RNA was extracted from cultured PBMCs using the RNeasy Plus Mini kit (Qiagen). cDNA was synthesised from the extracted RNA using the Transcriptor First Strand cDNA Synthesis kit (Roche) by following the manufacturer instructions. An additional no-RT control was included for each cDNA sample synthesised. The kinetic PCR amplification was carried out using the Viia7 Real-time PCR system (Applied Biosystems) with gene-specific primers and Fast SYBR Green Master Mix. The list of primers used is given in Supplementary table S2.

Chromatin Immunoprecipitation (ChIP)-qPCR

Up to 10 million cells were crosslinked with 1% formaldehyde for 10min at room temperature. Fixed cells were quenched with 125mM Glycine and lysed with Cell lysis buffer (5mM PIPES-KOH pH 8.0; 85mM KCl; 0.5% NP-40). Subsequently nuclei were pelleted by centrifugation at 2000rpm for 5 minutes and subjected to lysis with 130 µl Nuclear lysis buffer (1% SDS; 10mM EDTA; 50mM Tris-HCl pH8.0). Nuclear lysates were sonicated using the Covaris S220 sonicator in a microTUBE (Covaris), with the following Sonolab7.2 program parameters: Peak Incident Power: 105 Watts; Duty Factor: 10%; Cycles per burst:

200; Treatment time: 480 sec; Distilled Water Temperature: 4-6ºC. Sonicated lysates were subjected to immunoprecipitation (IP) using the following antibodies: ChIPAb+Trimethyl-Histone H3 Lys 4 (Millipore, 17-614) and ChIPAb+Trimethyl-Histone H3 Lys 36 (Millipore, 17-10032), ChIPAb+ Trimethyl-Histone H3 Lys 27 (Millipore, 17-622) and corresponding control IgG overnight at 4ºC in the presence of MagnaChIP A+G magnetic beads (Millipore). A 10% IP input sample was collected separately as a reference for relative quantification. The bead-bound immunoprecipitated DNA was washed sequentially for 10 minutes each at 4ºC with the following wash buffers- Low salt wash buffer (0.1% SDS; 1% Triton X-100; 2mM EDTA; 20mM Tris-HCl pH8.0; 150mM NaCl), High salt wash buffer (0.1% SDS; 1% Triton X-100; 2mM EDTA; 20mM Tris-HCl pH8.0; 500mM NaCl), LiCl wash buffer (0.25M LiCl; 1% NP-40; 1% Deoxycholic acid (sodium salt); 1mM EDTA; 10mM Tris-HCl pH8.0) and 2 washes with TE buffer (1mM EDTA; 10mM Tris-HCl pH8.0). The DNA was eluted from the beads by IP elution buffer (1% SDS; 0.1 M NaHCO3). The eluted DNA was reverse cross-linked at 65ºC overnight in the presence of 300mM NaCl and thereafter subjected to proteinase K digestion at 45ºC for 2 hours. The immunoprecipitated and input DNAs were purified by using the QIAquick PCR Purification Kit (Qiagen). The DNA enrichment in ChIP samples was quantified using region-specific primers for 5'-LTR junction, *Gag, Pol, Env, vCTCF, Tax* and 3'-LTR junction of the HTLV-1 provirus and corresponding qPCR TaqMan probes (sequences described in Supplementary table S2). The kinetic PCR amplification was carried out using the Viia7 Real-time PCR system (Applied Biosystems) with TaqMan Gene Expression Master Mix (ThermoFisher Scientific).

Methylated DNA Immunoprecipitation (MeDIP)

Genomic DNA from PBMCs was extracted using a QIAamp DNA Mini kit (Qiagen), following the manufacturer's instructions. The extracted DNA was sonicated using a Covaris S220 machine (Sonolab 7.2 program: Peak Incident Power: 175 Watts; DutyFactor: 10%; Cycles per burst: 200; treatment time: 105 sec; Distilled Water Temperature: 5-8ºC). MeDIP

assays were carried out using the MethylCollector Ultra kit (Active Motif) according to the manufacturer's protocol. Immunoprecipitated DNA was quantified by qPCR as described above for ChIP, using the same primers and probes.

Metabolomics protocol

Sample preparation: PBMCs isolated from HTLV-1 infected individuals were cultured overnight in the presence of 0.5mM DMOG or DMSO (control). Briefly, pelleted cells were lysed with ice-cold 80% methanol (MS grade). 0.2ml of each lysate was then filtered using a 10kd molecular weight cut-off filter (Amicon Ultra, Millipore). The liquid which had passed though the filter was then placed in an autosampler vial (Waters) and stored at -80^{o}C. On the day of analysis the extract was allowed to warm to 4^{o}C in the chilled autosampler and then analysed directly by LC/MS/MS.

LC/MS/MS: Metabolite analyses were performed using a Thermo Scientific ICS-5000+ ion chromatography system coupled directly to a Q-Exactive HF Hybrid Quadrupole-Orbitrap mass spectrometer with a HESI II electrospray ionisation source (Thermo Scientific, San Jose, CA). The ICS-5000+ HPLC system incorporated an electrolytic anion generator (KOH) which was programmed to produce an OH- gradient from 5-100mM over 37 minutes. An inline electrolytic suppressor removed the OH- ions and cations from the post-column eluent prior to eluent delivery to the electrospray ion source of the MS system (Thermo Scientific Dionex AERS 500). A 10 µL partial loop injection was used for all analyses and the chromatographic separation was performed using a Thermo Scientific Dionex IonPac AS11-HC 2 × 250 mm, 4 µm particle size column with a Dionex Ionpac AG11-HC 4 µm 2x50 guard column inline. The IC flow rate was 0.250 mL/min. The total run time was 37 minutes and the hydroxide ion gradient comprised as follows: 0mins, 0mM; 1min, 0mM; 15mins, 60mM; 25mins, 100mM; 30mins, 100mM; 30.1mins, 0mM; 37mins, 0mM. Analysis was performed in negative ion mode using ascan range from 80-900 and resolution set to 70,000. The tune file source parameters were set as follows: Sheath gas flow 60; Aux gas flow 20;

Spray voltage 3.6; Capillary temperature 320; S-lens RF value 70; Heater temperature 450. AGC target was set to 1e6 and the Max IT value was 250ms. The column temperature was kept at 30°C throughout the experiment. Full scan data were acquired in, continuum mode across the mass range m/z 60-900.

QUANTIFICATION AND STATISTICAL ANALYSIS

Processing and statistical analysis of Metabolomics data

Data Processing: Raw data was processed using Progenesis QI for small molecules (Waters, Elstree, UK). Briefly this encompassed chromatographic peak alignment, isotope cluster recognition (peak picking) and compound identification. Identification of compounds in experimental samples was based on matching to an in-house library of authentic standards, using four measured parameters for each compound from the database. These were: accurate mass measurement (<5ppm) based on theoretical mass derived from the chemical formula, experimental retention time window of 0.5mins, isotope pattern recognition (calculated from chemical formula) and matching with fragmentation patterns from an authentic standard where these were available from survey scans. All values in the database were obtained from the analysis of authentic standard compounds.

Statistical Analysis: Statistical analysis was performed using Progenesis QI and the EZ info plugin for Progenesis QI developed by Umertrics. Supervised and unsupervised modelling of the data was performed (PCA and OPLS-DA). Volcano plots, S-plots and VIP values were extracted from OPLS-DA models to help identify highly significant compounds and potential biomarkers. P-values, %CV and fold-changes associated with the statistical comparison of experimental groups were calculated for each metabolite using progenesis QI. These data were used to identify and evaluate potential metabolic biomarkers. The identified metabolites were sorted according to the maximum fold difference in normalized abundance between

DMSO-treated and DMOG-treated samples respectively. Any difference in metabolite abundance, which was statistically significant ($p<0.05$), and fold change >1.3-fold, was analysed further. The resultant metabolite list was mapped according to the metabolic pathways they were associated with.

Quantification of qRT-PCR data

LinRegPCR-Ct method (Cikos et al., 2007) was used for relative quantification of target mRNA levels. LinRegPCR software was used to determine baselines, threshold and mean efficiency (E) of the reaction to calculate target mRNA quantity (R0), where R0 = Threshold/ E^{Ct}. All values were normalized to their respective 18S rRNA levels, which was the internal PCR control.

Quantification of ChIP-qPCR and MeDIP data

DNA enrichment was calculated as % Input = $(E^{\Delta Ct})*10$, where ΔCt= Ctinput- Ctsample. LinRegPCR software was used to determine the mean efficiency of the reaction for each primer pair.

Statistical Analyses

Two-tailed Student's T test, Wilcoxon matched pairs signed rank test and 1-way ANOVA with post-test for linear trend were employed for statistical analysis of data as described in the corresponding figure legends.

DATA AND SOFTWARE AVAILABILITY

The raw metabolomics data with the identified metabolites has been provided in Supplementary file S2.

SUPPLEMENTAL INFORMATION

File S1. List of patient blood samples used in this study. Related to all figures (1-6)

File S2. List of identified metabolites in response to DMSO (control) or DMOG treatment in primary PBMCs derived from HTLV-1 infected individuals. Related to figure 4

Figure 1

Click here to download Figure 2017-07-14 Kulkarni et al - Figure 1.jpg

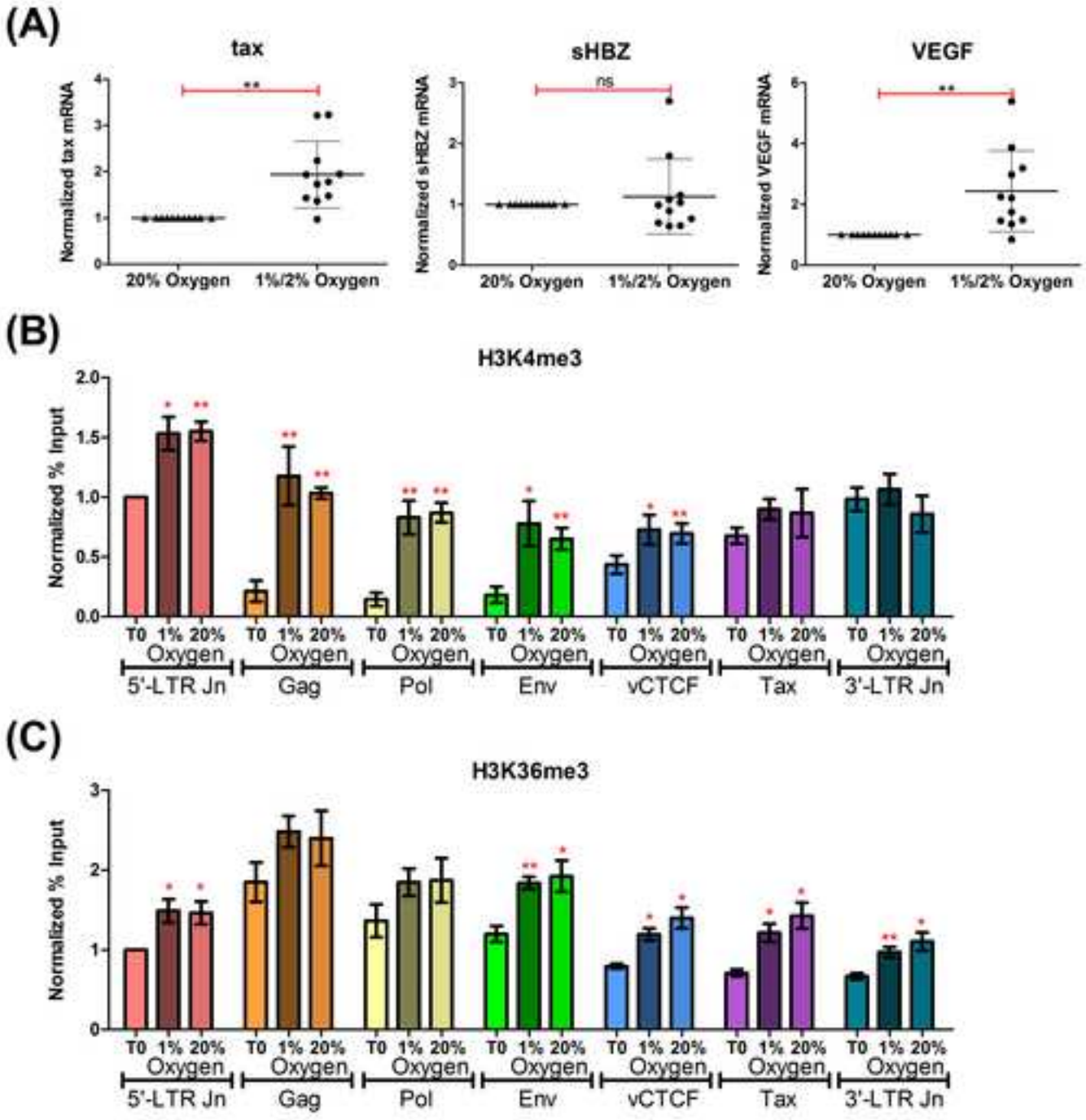


Figure 2

Click here to download Figure 2017-07-14 Kulkarni et al - Figure 2.jpg

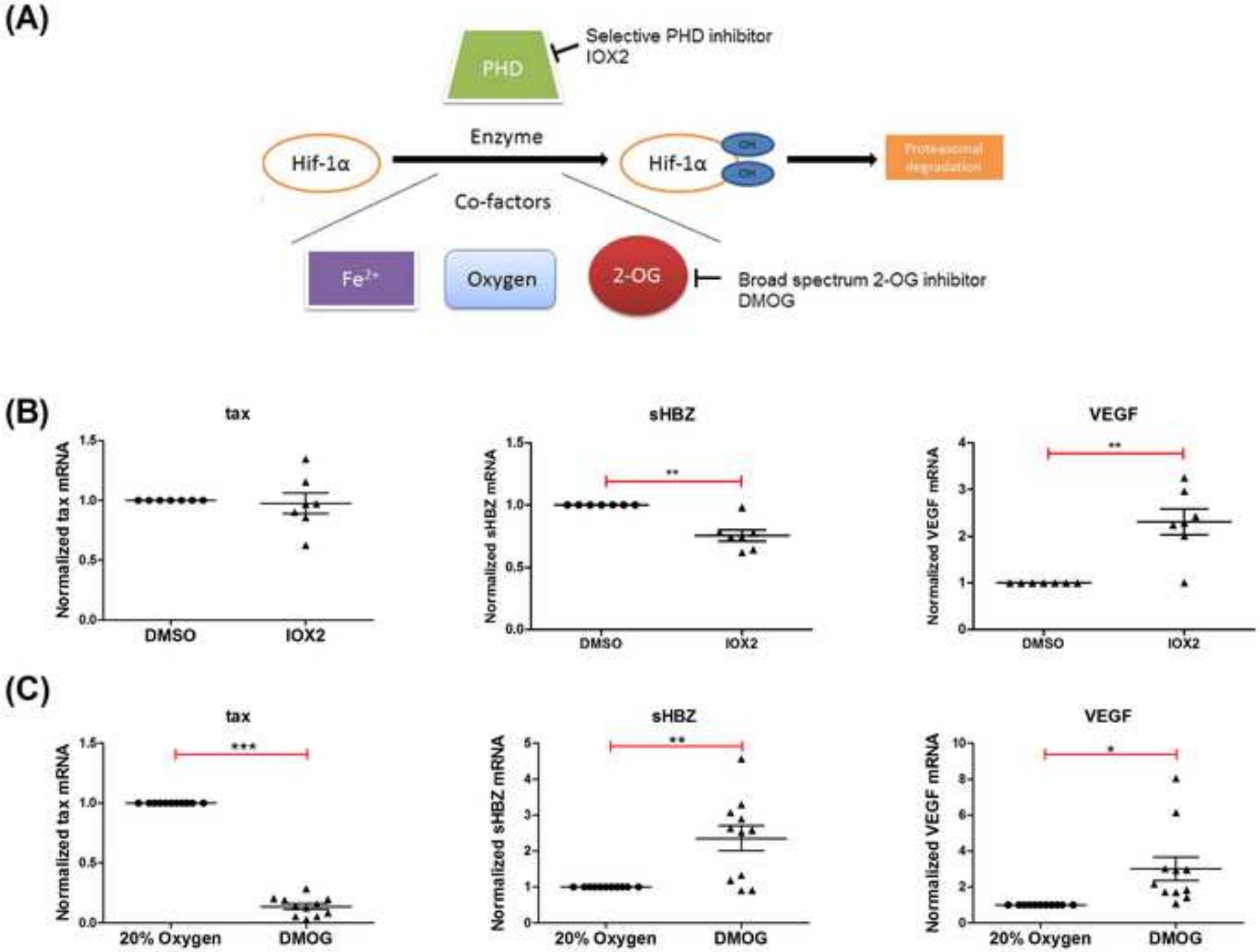


Figure 3

Click here to download Figure 2017-07-14 Kulkarni et al - Figure 3.jpg

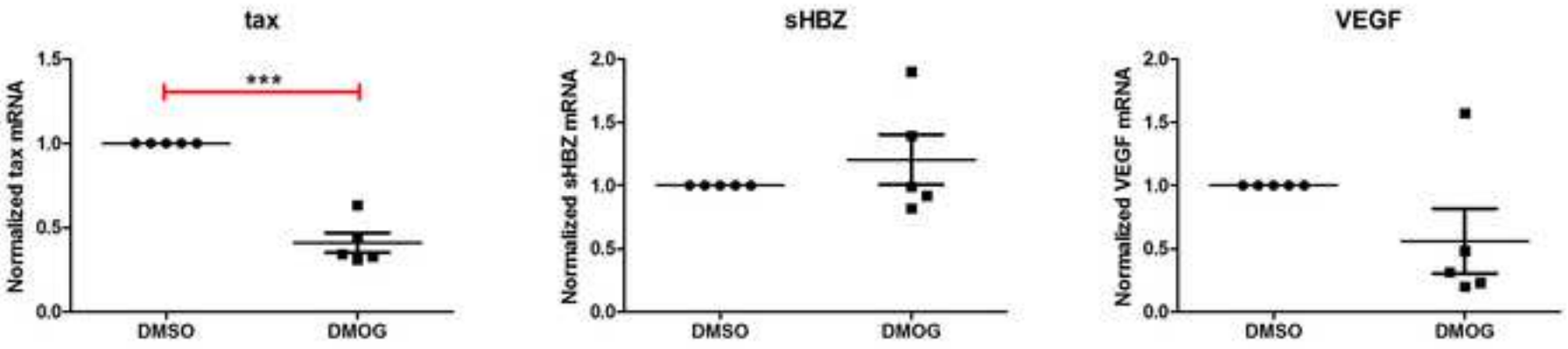


Figure 4

Click here to download Figure 2017-07-14 Kulkarni et al - Figure 4.jpg

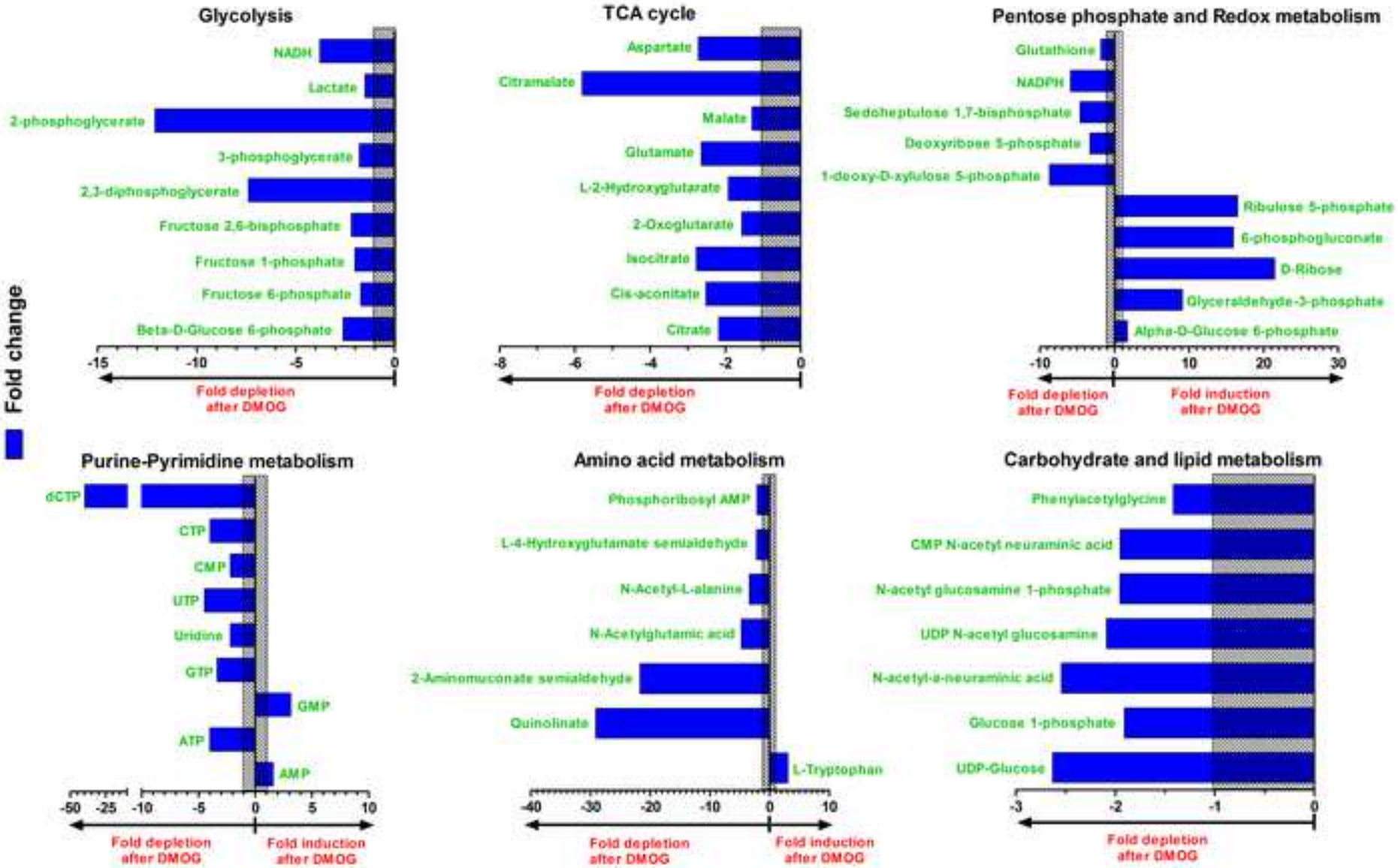


Figure 5

Click here to download Figure 2017-07-14 Kulkarni et al - Figure 5.jpg

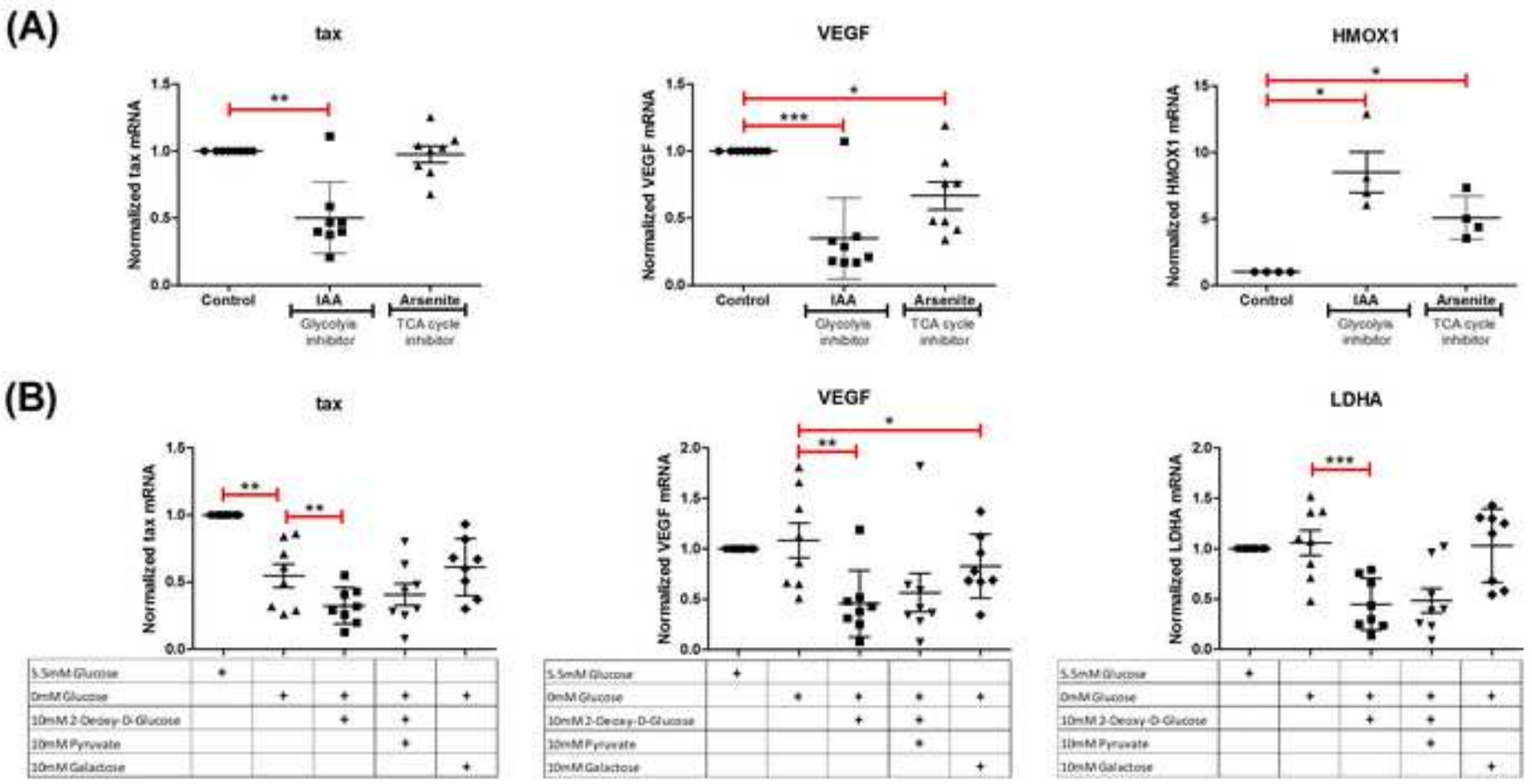
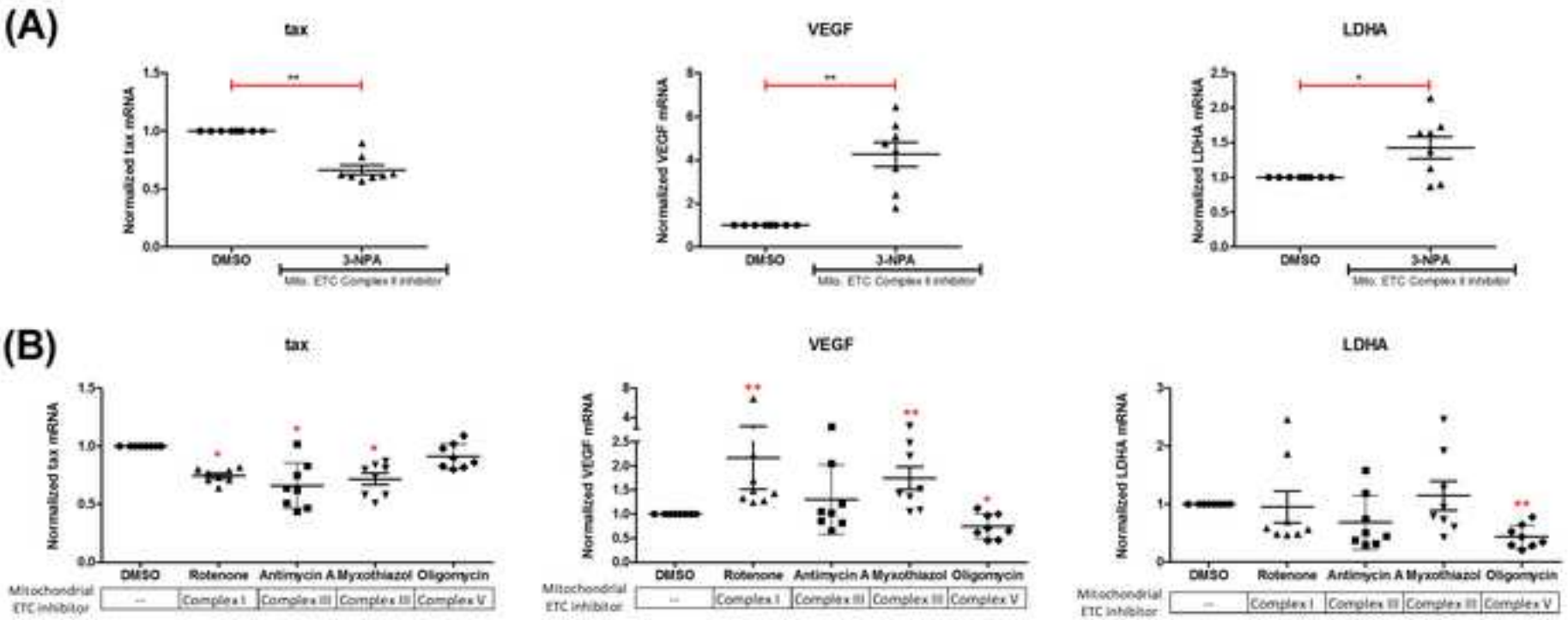


Figure 6

Click here to download Figure 2017-07-14 Kulkarni et al - Figure 6.jpg



CellPress

TABLE FOR AUTHOR TO COMPLETE

Please upload the completed table as a separate document. ***Please do not add subheadings to the Key Resources Table.*** *If you wish to make an entry that does not fall into one of the subheadings below, please contact your handling editor. (****NOTE:*** *For authors publishing in Current Biology, please note that references within the KRT should be in numbered style, rather than Harvard.)*

KEY RESOURCES TABLE

REAGENT or RESOURCE	SOURCE	IDENTIFIER
Antibodies		
ChIPAb+Trimethyl-Histone H3 Lys 4	Millipore	Cat# 17-614
ChIPAb+Trimethyl-Histone H3 Lys 36	Millipore	Cat# 17-10032
ChIPAb+ Trimethyl-Histone H3 Lys 27	Millipore	Cat# 17-622
Bacterial and Virus Strains		
N/A	N/A	N/A
Biological Samples		
Human patient samples provided as excel file S1	NCHR	http://www.htlv1.eu/
Chemicals, Peptides, and Recombinant Proteins		
List of chemicals used provided in supplementary table S1	Refer to table S1	Refer to table S1
Critical Commercial Assays		
Methyl Collector Ultra kit	Active Motif	Cat# 55005
Deposited Data		
N/A	N/A	N/A
Experimental Models: Cell Lines		
N/A	N/A	N/A

Experimental Models: Organisms/Strains		
N/A	N/A	N/A
Oligonucleotides		
List of oligonucleotides and probes used provided as supplementary table S2	Refer to table S2	Refer to table S2
Recombinant DNA		
N/A	N/A	N/A
Software and Algorithms		
LinRegPCR- qPCR analysis software	HFRC, Netherlands	http://www.gene-quantification.com/LinRegPCR_help_manual_v11.0.pdf
Progenesis QI	Waters, U.K.	http://www.waters.com/waters/en_US/Progenesis-QI-Software/nav.htm?cid=134790655&locale=en_US
Other		
N/A	N/A	N/A

Glucose metabolism and oxygen availability govern reactivation from latency of the human retrovirus HTLV-1

Supplemental information

Supplementary figures S1 to S4

Supplementary tables S1 and S2

Figure S1. Related to Figure 1

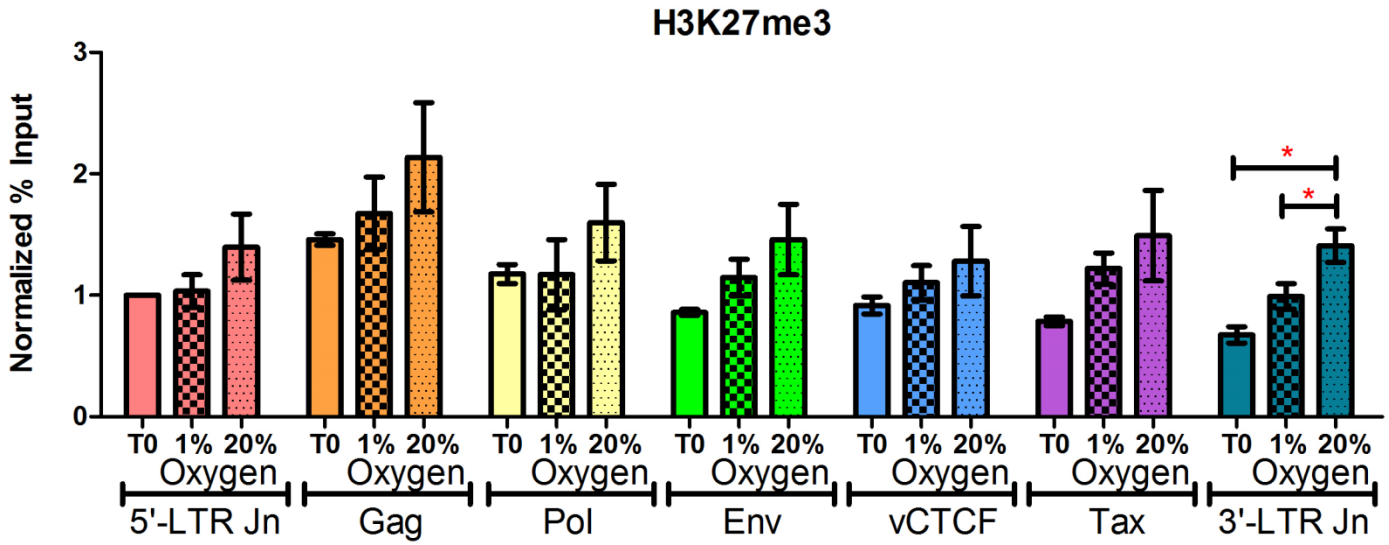


Figure S1: H3K27me3 status changes in the HTLV-1 provirus upon reactivation under physiological (1%) hypoxia or normoxia. HTLV-1-infected PBMCs were either fixed immediately (T0) or cultured under hypoxia (1% oxygen) or normoxia (20% oxygen) overnight and subsequently fixed and subjected to ChIP with antibodies directed against H3K27me3 and IgG, and primers specific for the 5'-LTR Jn, *Gag*, *Pol*, *Env*, *vCTCF*, *Tax* and 3'-LTR Jn of the HTLV-1 provirus. Enrichment is expressed as % input DNA and normalized to T0 at the 5'-LTR junction. Error bars represent the standard error of 4 independent ChIP experiments. Statistical significance was calculated using the two-tailed Student's T-test where * represents $p<0.05$.

Figure S2. Related to Figure 2

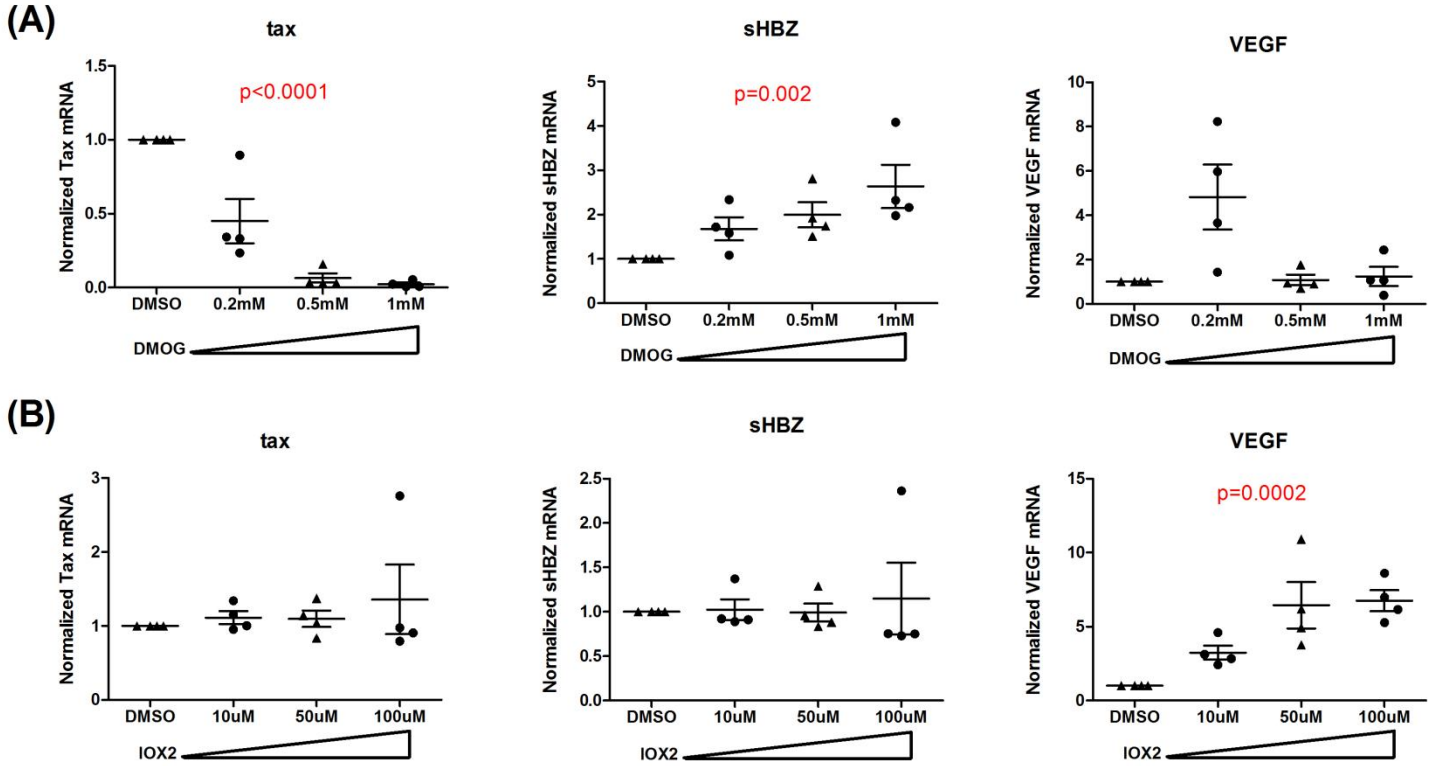


Figure S2: Dose-response effects of DMOG and IOX2 on HTLV-1 transcription. HTLV-1-infected primary PBMCs were treated overnight with increasing concentrations of DMOG **(A)** or IOX2 **(B)**. RNA was extracted and subjected to RT-qPCR with primers specific for *tax* mRNA (plus-strand), *sHBZ* (minus-strand) or *VEGF* mRNA (positive control). Error bars represent the standard error of the mean (n=4). Statistical significance was calculated using 1-way ANOVA test with post-test for linear trend. P-values < 0.05 are significant.

Figure S3. Related to Figure 2

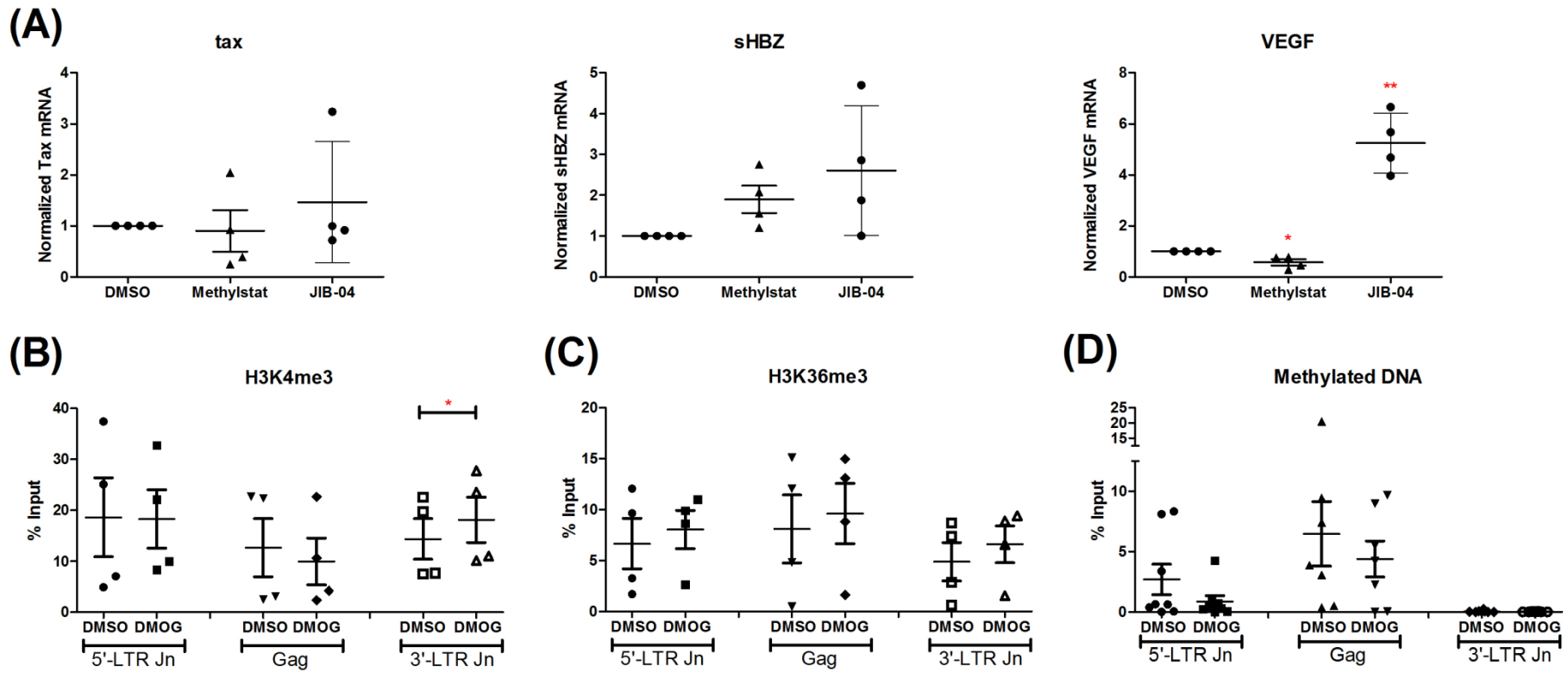


Figure S3: 2-OG oxygenases do not control plus-strand HTLV-1 transcription. (A) HTLV-1-infected primary PBMCs were treated overnight with either the broad spectrum JmjC KDM inhibitors Methylstat, JIB-04, or a DMSO control. RNA was extracted and subjected to RT-qPCR with primers specific for *tax* mRNA (plus-strand), *sHBZ* (minus-strand) or *VEGF* mRNA (positive control). Error bars represent the standard error of the mean (n=4). Statistical significance was calculated using the two-tailed Student's T-test where * represents $p<0.05$ and **

represents p<0.005. **(B, C) Epigenetic (histone methylation status) changes at the HTLV-1 provirus following DMOG treatment.** HTLV-1-infected PBMCs were cultured overnight with either DMOG or DMSO (control) and subsequently fixed and subjected to ChIP-qPCR with antibodies directed against H3K4me3, H3K36me3 and IgG and primers specific for the 5'-LTR Jn, *Gag* and 3'-LTR Jn of the HTLV-1 LTR. Enrichment is expressed as % input DNA. Error bars represent the standard error of 4 independent ChIP experiments. Statistical significance was calculated using the two-tailed Student's T-test where * represents p<0.05. **(D) Effect of DMOG treatment on DNA cytosine methylation within the HTLV-1 provirus.** HTLV-1-infected PBMCs were cultured with either DMOG or DMSO (control) overnight. Genomic DNA was isolated, sonicated and subsequently subjected to Methylated DNA Immunoprecipitation using the Methyl Collector Ultra kit (Active Motif) and primers specific for the 5'-LTR Jn, *Gag* and 3'-LTR Jn of the HTLV-1 LTR. Enrichment is expressed as % input DNA. Error bars represent the standard error of the mean for the 5'-LTR & 3'-LTR regions (n=8), and for the Gag region subjected to MeDIP (n=7).

Figure S4. Related to Figures 5 and 6

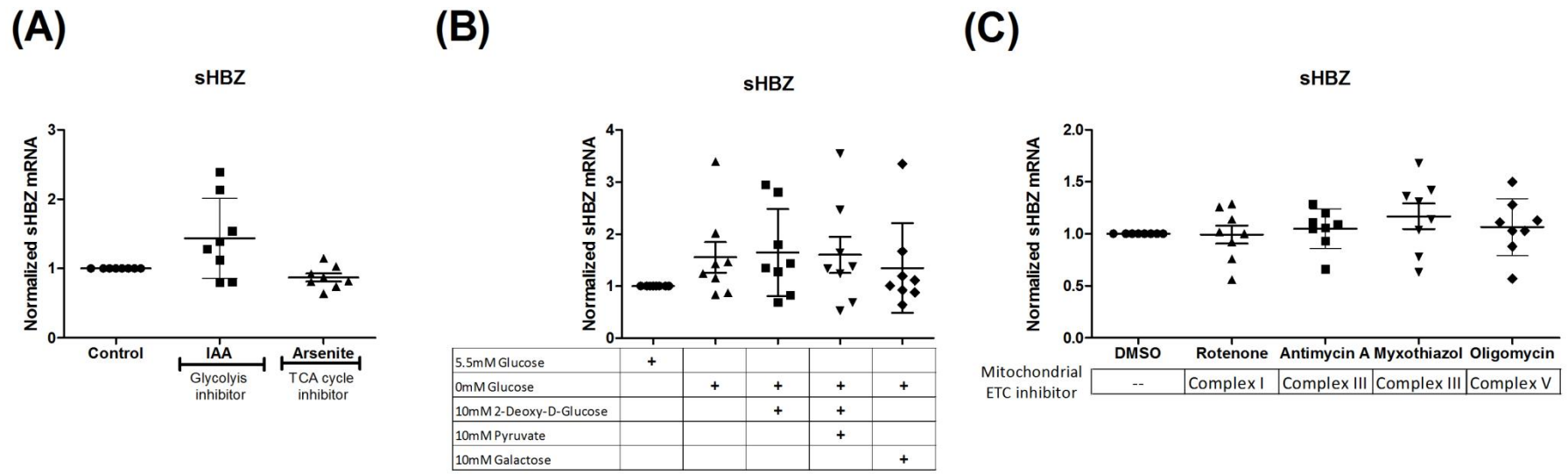


Figure S4: Glucose metabolism and the mitochondrial electron transport chain do not govern minus-strand HTLV-1 transcription. HTLV-1-infected primary PBMCs were treated overnight with control (water), iodoacetic acid (IAA) or sodium arsenite **(panel A)** or cultured under indicated concentrations of glucose-containing RPMI in the presence or absence of the glycolysis inhibitor 2-deoxy-D-glucose (2-DG) & TCA cycle inducers sodium pyruvate and galactose **(panel B)** or cultured with the indicated mitochondrial ETC inhibitors **(panel C)**. RNA was extracted and subjected to RT-qPCR with primers specific for *sHBZ* mRNA (minus-strand). Error bars represent standard error of the mean (N=8). Statistical significance was calculated using the two-tailed Student's T-test where * represents $p<0.05$.

Table S1. Chemical compounds list. Related to all figures (1-6)

Sr. No.	Name	Supplier	Solvent	Final conc.	Mechanism of action	Ref
1	DMOG	Cayman Chem.	DMSO	0.5mM	Broad spectrum 2-OG oxygenase inhibitor	(Jaakkola et al., 2001)
2	IOX2	Cayman Chem.	DMSO	50µM	Selective PHD inhibitor	(Chowdhury et al., 2013)
3	Iodoacetic acid (IAA)	Sigma	Water	20µM	Glycolysis inhibitor, ROS inducer	(Sabri and Ochs, 1971)
4	Sodium Arsenite	Courtesy: CJS	Water	1µM	TCA cycle inhibitor, ROS inducer	(Bergquist et al., 2009)
5	2-Deoxy-D-Glucose	Sigma	Water	10mM	Glycolysis inhibitor	(Zhong et al., 2009)
6	Sodium Pyruvate	Life tech.	Solution	10mM	TCA cycle inducer	(Diers et al., 2012)
7	Galactose	Sigma	Water	10mM	Oxphos inducer	(Aguer et al., 2011)
8	3-Nitropropionic acid	Courtesy: CJS	DMSO	1mM	ETC Complex 2 inhibitor	(Rohlena et al., 2013)
9	Rotenone	Sigma	Chloroform	10µM	ETC Complex 1 inhibitor	(Rohlena et al., 2013)
10	Antimycin A	Sigma	DMSO	10µM	ETC Complex 3 inhibitor	(Rohlena et al., 2013)
11	Myxothiazol	Sigma	DMSO	10µM	ETC Complex 3 inhibitor	(Rohlena et al., 2013)
12	Oligomycin	Sigma	DMSO	10uM	ATP synthase (ETC Complex V) inhibitor	(Rohlena et al., 2013)
13	Methylstat	Sigma	DMSO	10µM	JmJc Histone Demethylase inhibitor	(Luo et al., 2011)
14	JIB-04	Sigma	DMSO	2µM	JmJc Histone Demethylase inhibitor	(Wang et al., 2013)

Table S2. List of primers and probes used for qRT-PCR, ChIP-qPCR and MeDIP. Related to all figures (1-6)

Sr. No	Gene	Orientation	Sequence	
qRT-PCR				
1	Tax	F	5′-CCGGCGCTGCTCTCATCCCGGT-3′	(Satou et al., 2016)
		R	5′-GGCCGAACATAGTCCCCCAGAG-3′	
2	sHBZ	F	5′-GGACGCAGTTCAGGAGGCAC-3′	
		R	5′-CCTCCAAGGATAATAGCCCG-3′	
3	18S rRNA	F	5′-GTAACCCGTTGAACCCCATT-3′	
		R	5′-CCATCCAATCGGTAGTAGCG-3′	
4	VEGF	F	5'-GACTCCGGCGGAAGCAT-3'	(van Kuijk et al., 2016)
		R	5'-TCCGGGCTCGGTGATTTA-3'	
5	HMOX1	F	5′-CTCAAACCTCCAAAAGCC-3′	(Reichard et al., 2007)
		R	5′-TCAAAAACCACCCCAACCC-3′	
6	LDHA	F	5′-TTGGTCCAGCGTAACGTGAAC-3′	(Allison et al., 2014)
		R	5′-CCAGGATGTGTAGCCTTTGAG-3′	
ChIP-qPCR and MeDIP				
				(Satou et al., 2016)
1	5'-LTR Junction	F	5′-GACAGCCCATCCTATAGCACTC-3′	
		R	5′-CTAGCGCTACGGGAAAAGATT-3′	
2	Gag	F	5′-CAGAGGAAGATGCCCTCCTATT-3′	

		R	5′-GTCAACCTGGGCTTTAATTACG-3′
3	Pol	F	5'-CAGCCCATTCGGCAAG-3'
		R	5'-TGAGAGTAGTAGTAGGTCCTCATGG-3'
4	Env	F	5'-GCTAGTTCTGCCCAGTGGAT-3'
		R	5'-TTGGTGGTCTTTTTCTTTGG-3'
5	vCTCF	F	5'-CCGATCACGATGCGTTTC-3'
		R	5'-ACGGTTTGCTATCCTTAGAAGA-3'
6	Tax	F	5'-CTCCTTCCGTTCCACTCAAC-3'
		R	5'-GTGGTAGGCCTTGGTTTGAA-3'
7	3'-LTR Junction	F	5′-AATACACCAACATCCCCATTTC-3′
		R	5′-GTTTTTCACTGGGAGGCTCTAA-3′

(Satou et al., 2016)

qPCR Probes (ChIP-qPCR and MeDIP)			
1	5'-LTR Junction		FAM -TCGTCCGGGATACGAGCGCC- TAM
2	Gag		FAM -TACCGTTAGATCCCGCCCGTCG- TAM
3	Pol		FAM- CATGGATGACATTCTCCTAGCAAGCCC -TAM
4	Env		FAM-CTGCATGCCCAAGACCCGTCG-TAM
5	vCTCF		FAM-TGGAGGGCCCCGTCGCA-TAM
6	Tax		FAM-CGCCTATGATTTCCGGGCCCTG-TAM
7	3'-LTR Junction		FAM -AGAGGCAGATGACAATGACCATGAGCC-TAM



Click here to access/download

Supplemental Movies and Spreadsheets

Suppl File S1-Patient samples list.xlsx



Click here to access/download

Supplemental Movies and Spreadsheets

Suppl file S2-Metabolomics data.xlsx